

2013

OPTIMAL MANAGEMENT OF CORROSION AND ODOUR PROBLEMS IN SEWER SYSTEMS (ARC LP0882016)

SP8: Model-based tool for decision support for technology selection, prioritization and optimization

Draft Final Report

This is the draft version of the final report summarizing the key findings of SP8 of SCORe project. Australian Research Council (ARC) through an ARC Linkage Project (ARC LP0882016) funded the project. A number of industry partners participated in the subproject and contributed to its funding.

**Advanced Water Management Centre
The University of Queensland**

November 2013

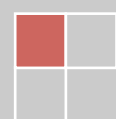


TABLE OF CONTENTS

Table of Contents	2
Executive Summary	4
1. Introduction	7
1.1. Background	7
1.2. Objectives of the Sub-project.....	7
1.3. About This Report.....	8
2. Expected Outcomes and Benefits.....	9
3. Summary of Outcomes.....	9
3.1. Impacts of Trade Waste	9
3.1.1. Brewery Wastewater	9
3.1.2. Dairy Wastewater.....	12
3.2. Modeling of Methane Production in Sewers	15
3.3. Modeling of Impacts of pH on Sulfide and Methane Production.....	18
3.4. Impacts of Flow Velocity on Sulfide Production	22
3.5. Effects of Sewer Sediments on H ₂ S Production	26
3.6. Modeling of H ₂ S Transfer in Sewer Pipes.....	31
3.6.1. Methodology	31
3.6.2. Results	33
3.7. Modeling of H ₂ S Transfer in Critical Structures	35
3.7.1. Background	35
3.7.2. Inverted Siphons	35
3.7.3. Drop Structures	36
3.7.4. Discharge Manholes.....	36
3.7.5. Other Structures.....	37
3.8. Modeling of H ₂ S Transfer in Drop Structure	37
3.8.1. Model Description	37
3.8.2. Simulation Results.....	39
3.9. Ferric Inhibition to Sewer Biofilm.....	40
3.9.1. Background	40



3.9.2. Field Study	40
3.9.3. Results	41
3.10. Modeling of H ₂ S Consumption in Sewer Biofilm	44
3.10.1. Background.....	44
3.10.2. Empirical Model.....	44
3.10.3. Fundamental Model	46
3.11. Sewer Modeling	48
3.11.1. Identification of Key Model Parameters	48
3.11.2. Sewer Model Updates.....	49
3.11.3. Impacts of Chemical Dosing	49
3.11.4. Data Import/Export Interface	49
3.11.5. Calibration of Key Model Parameters	50
3.11.6. Air Transport Modeling.....	51
3.12. Model Case Studies	52
3.12.1. Queensbury Sewer System, SA Water.....	52
3.12.2. NSOOS Sewer System, Sydney Water.....	54
3.12.3. Veolia Water Sewer, France	54
4. References.....	57

EXECUTIVE SUMMARY

This research work on “Optimal management of corrosion and odour problems in sewer systems” is jointly undertaken by the Advanced Water Management Centre at The University of Queensland (AWMC-UQ) along with 3 other universities, and 15 industry partners, which included major water utilities in Australia. The Australian Research Council (ARC) with additional cash and in-kind contribution from the industry partners jointly funded the project. The cash budget was approximately \$8.1m including \$4.7m cash contribution from the ARC. Additionally, all partners involved including the Universities also made substantial in-kind contributions to the project.

The project is divided into 4 themes namely (1) understanding and predicting corrosion processes; (2) gas phase technologies; (3) liquid phase technologies; and (4) decision support and knowledge management. Each of the themes consist of a number of sub-projects. This subproject (SP8) aimed to develop model-based tool for decision support for technology selection, prioritization and optimization by combining laboratory and field works and mathematical modeling. The subproject was started in 2009 and was completed on 2013.

The subproject delivered strong outcomes with most milestones achieved as planned. The knowledge and model generated are being applied by the participating industry partners for the management of their sewer systems, both rising and gravity mains.

The main outcomes of the project are summarised below.

- Study revealed that the addition of brewery wastewater in general affects the performance of the sewer system with respect to both sulfide and methane production. The introduction of brewery wastewater has two impacts: decrease of pH; and increase in VFA levels. Both of these changes are expected to influence the microbial activity in the system. In the short-term exposition test, introduction of brewery wastewater increased the rates of sulfide and methane production at a constant pH. The sulfide production rate decreased with increased proportion of brewery wastewater, while the methane generation rate increased. In the long-term exposition test with 10% brewery wastewater, higher sulfide and methane production rates as compared to the reference system were observed. When the proportion of brewery wastewater was further increased to 25%, the sulfide generation rate decreased, but opposite was the case with methane production.
- Study revealed that the addition of dairy wastewater affected sulfide and methane generation in a laboratory sewer system. Significant increase in COD concentration and decrease in pH were observed in reactors dosed with dairy WW. The addition of 10% v/v dairy wastewater resulted in the decrease of sulfide and methane production rates by up to 30% and 10%, respectively. These results are different from those observed with brewery wastewater. No significant change in activity was observed in the latter case despite low pH. A number of postulations are made for the decreased activity and possible causes include: slow biodegradation of dairy waste due to slow hydrolytic step of fat degradation, production of some inhibitory compounds during fat degradation, and absorption of fat to the biofilm surface thereby affecting substrate transfer to the biofilm.



- A simple conceptual model for methane formation in rising main sewers can successfully describe the experimental methane and sulfide data observed at either a lab-scale sewer system or at a real sewer. However, more field data are needed to more accurately calibrate the model parameters. Kinetic calibration shows that MA are more competitive than SRB in sewer biofilms for common electron donors (H_2 and acetate). The mass transfer limitation of sulfate from the bulk liquid phase to the biofilms is likely responsible for this observation.
- Sediments show variable characteristics as a function of the sewer location and wastewater composition. Sulfate reduction and methane production processes under stagnant flow conditions are diffusion limited and these have little contribution to over sulfide and methane production in sewers. Sulfate reduction process is an areal process and thus water flow velocity affects the rate. On the other hand, methane production is a volumetric process and both exogenous and endogenous soluble carbon sources can be utilized and converted to methane. Flow velocity does not affect the methane production rate. Contributions of the sediments to overall sulfate reduction and methane production in sewers are significant and comparable to that of biofilm processes.
- Both the simulation and the experiment results demonstrated significant impacts of flow velocity and hence the shear stress on the rate of sulfate reduction by sewer biofilm, especially under low flow velocity. The sulfate reduction rate increased in general with the increase in the shear stress. The increase was significant when the shear stress was below 0.5 Pa. Beyond this; the increase in velocity had only minor impacts. The results of this study further highlighted the need for considering the effect of flow on sulfide production rate in sewer models for the accurate prediction of sulfide generation.
- The impact of pH on sulfidogenesis by anaerobic sewer biofilm was studied and a model to predict this impact was developed, calibrated and validated. Sulfate reduction rate by sewer biofilms vary with pH, reaching its maximum in the neutral pH range (6.5-7.5). The rate decreases with the shift of pH away from this range, reaching approximately 50% of the maximum rate at pH 4.0 and 9.0. Free ammonia likely plays an important role in the inhibitory effects in the alkaline pH range, where the direct effect of pH is not obvious. The inhibition of sulfate reduction at a pH higher than the neutral range could be adequately modeled as free ammonia inhibition. Inhibition of sulfate reduction by sewer biofilm under acidic pH conditions is likely caused by the low pH itself rather than by the inhibitory effects of H_2S or organic acids. The inhibition of sulfate reduction at a lower pH could therefore be modeled as pH inhibition.
- Nine different models recommended for modelling liquid-gas transfer of H_2S in gravity sewer pipe were tested for their ability to predict the transfer rates measured in a laboratory gravity sewer system under a number of conditions with respect to pipe slope, flow rate and pipe diameter. A comparison of the measured and estimated transfer rate revealed that the models proposed by Krenkel and Orlob (1962), Taghizadeh-Nasser (1986) and Balmer and Tagizadeh-Nasser (1995) could best reproduce the results.
- Methodologies for including various key sewer structures affecting liquid-gas transfer of H_2S have been proposed.



- Ferric inhibition to sewer biofilm was investigated through a field study conducted on Bellambi Sewer System of Sydney Water, which is receiving ferrous dosing for a number of years. Despite some indication of reduced sulfide and methane formation in the sewer pipe, the results were somewhat inconclusive owing to the variability of the results, limited amount of data available and lack of baseline data.
- An empirical model in the form of a power function is proposed for modelling H₂S consumption by the biofilm in sewer crown. The model was developed and validated using the data collected in SP1 of the SCORe project.
- A number of model components have been included into the SeweX model resulting in significant improvement of the model. Key model parameters requiring calibration are identified and the method for their calibration is proposed. In addition, an air transport model proposed in SP4 has been adapted to predict airflow in gravity sewer pipes.
- The SeweX model enhanced with additional model components was applied to three sewer systems, two in Australia and one in France to demonstrate its capability to predict H₂S in both liquid and gas phase and its application in optimising chemical dosing. Sydney Water undertook the model application to NSOOS sewer system.
- Information collected in this sub-project has been provided to SP9 for developing SCORe knowledge management system.



1. INTRODUCTION

1.1. BACKGROUND

The UQ Sewer Model (SeweX) has been demonstrated to predict liquid level H₂S concentration at various sewer systems in Australia very well. The focus of the UQ Sewer Model currently so far has been the prediction of H₂S in liquid phase. Through the ARC linkage project completed prior to the start of the current project, we gained additional knowledge on the biotransformation processes in sewer system, and identified some key enhancement required for the current sewer model. The current model does not include methane production and the effects of sewer sediment on overall H₂S production rate. In addition, the impact of different trade wastes, mainly differing in organic strength and composition, on H₂S production is largely unknown.

The release of H₂S to the sewer and the ambient atmosphere has direct impact in corrosion and odour problems. The hydrodynamics of the air flow in a sewer is complex and greatly affects the release of H₂S. To address the problem of corrosion and odour due to H₂S production, the assessment of the effectiveness of any H₂S control measure should be based on gas phase H₂S concentration rather than the liquid phase one. It is essential that the dynamics of the air flow is accurately predicted and integrated into current sewer model. A simplified and generalized air-transport model capable of adequately describing the process should be integrated with the liquid-phase H₂S prediction model.

Since the sulfate reducing bacteria and methane producing bacteria compete for the same substrate (organic matter), methane production could influence the sulfide generation. However, the consequences of methane production in sulfide generation and the effectiveness of H₂S control methods such as oxygen and nitrate injection are mostly unknown at this stage. It is important that the production of CH₄ be included in the sewer model so that carbon balance could be closed and also the release of CH₄ (a potent green house gas) into atmosphere of our sewer networks could be accurately estimated

The focus of current UQ model is the prediction of sulfide concentration in liquid phase. Also, the key enhancements identified in this project, which are thought to improve the capability and expand the scope of the model, have not been implemented yet. Since the problem of odour and corrosion is related to gas-phase H₂S concentration, for the model to better serve as the management tool, it should be able to predict H₂S transfer to and transport in the gas phase accurately.

In this proposed research work, we are aiming to extend the current model to predict gas phase H₂S transfer and transport relevant to gravity sewer system. This would help to link the model outputs to other models such as corrosion and odour models so that the cause-effect relationships could be realistically investigated.

1.2. OBJECTIVES OF THE SUB-PROJECT

This sub-project aims to provide wastewater industry with a model-based tool for the assessment of the odor potential and the service life of existing sewer systems. The tool developed in this sub-project will enable the water authorities to identify the locations most vulnerable to sulfide attack (hot-spots), to predict the impact of various corrosion and odour mitigation strategies on sulfide control; and to optimize their efforts in accordance to the specific conditions of a given sewer network. This is expected to serve as a very useful



planning tool for operation and maintenance of sewer system and to form a part of the Decision Support System.

To achieve the above objective, the following aspects of the existing model will be enhanced through field and laboratory studies:

1. Gas phase transport, which depends upon: (i) liquid-gas mass transfer rate; (ii) water velocity; (iii) site conditions; and (iv) the ventilation technology employed. The field data and information collected in Subproject 4 (SP4) will be used for this purpose.
2. Improvement of the modeling of carbon transformation in rising main
3. The contribution of sewer sediments to sulfide production
4. The effect of flow velocity on sulfide production
5. The effects of trade waste discharge on sulfide production and pH change
6. Modeling the sulfide removal in the gas phase by the sewer biofilms based on results obtained in Sub-project 1 (SP1).

In addition to these, the following tasks will also be conducted.

1. Enhancement of model application and functionality through better user interface, manuals and training.
2. Model calibration protocol. Accurate predictions in a sewer system are possible only if the model is calibrated properly. In this project, we will also develop specific methods for the calibration of the most important kinetic parameters and document the calibration procedure. These methods will be developed based on the results of experiments to be conducted on in-situ biofilm samples directly collected for actual sewer pipes and field data. It will provide industry partners tools for developing models for their own sewer networks.
3. Case studies for model application.

Further, the sewer model will be integrated with hydraulic model (for flow rate, velocity and flow depth), air-transport model to be developed in SP4, and corrosion model to be developed in SP1. Simple user interfaces/methodologies to link the sewer model with each of these external models will be developed.

1.3.ABOUT THIS REPORT

This report is written to summarise the main conclusions of the research, rather than to provide a complete description of all the tasks/activities undertaken during the project. It is structured in such a way that each section is dedicated to a particular conclusion/outcome. Whenever necessary, key experimental evidence is presented to support the conclusions. The summary of the project outcomes is preceded with sections documenting the project methodology/research plan and the key materials and methods.

During the course of the project (June 2009 and February 2013), 8 Detailed Project Reports were produced which contained all the technical details of the project. Readers are referred to these reports for detailed scientific and technical information arising from the project.

2. EXPECTED OUTCOMES AND BENEFITS

The followings outcomes and benefits are expected from the sub-project.

1. A model-based tool to support industry to:
 - Assess sulfide production potentials of their sewer networks, and identify the locations most vulnerable to sulfide attack (hot spots);
 - Predict the impact of various corrosion and odour mitigation strategies including both chemical additions and ventilation technologies on sulfide control; and
 - Support optimizing the use of these strategies by selecting the most suitable technologies in accordance to the specific conditions of a given sewer network, identifying the most desirable locations for chemical dosage (or ventilation) and the optimal dosage rates.
2. A calibrated model, with user-friendly end-user interface, for each of the testing sites selected by the participating industry partners, delivered to industry partners in executable code.
3. Industry staff trained for the use of the model.
4. A protocol for the calibration of the sewer model.
5. One PhD graduate to serve Australian wastewater industry.
6. General guidelines and for the use of chemical addition and others such as ventilation technology in terms of efficiency to ensure H₂S targets are met whilst minimizing both costs and downstream effects.
7. Cost benefit assessment thorough the case studies.
8. Information for updating the SCoRe knowledge management system

3. SUMMARY OF OUTCOMES

3.1. IMPACTS OF TRADE WASTE

Brewery and dairy wastewaters were selected as the two trade wastes to be studied for their impacts on sulfide generation and other biological processes in sewer system. The main objective of this study was to investigate the effects of brewery and dairy waste waters on sulfide and methane production in sewer through experimental studies and to provide information for the development of relevant model components to characterize these impacts.

3.1.1. BREWERY WASTEWATER

A laboratory set-up consisting of two airtight reactors: experimental (R1) and control (R2) was used for the study. The control reactor was intermittently fed with sewage while the experimental reactor was dosed with a mixture of brewery and domestic wastewater at two different proportions (10 and 25% v/v). Each reactor system was exposed to 4 pump events per day with a hydraulic retention time (HRT) of 6 hours. To mimic the real condition of a



rising main, the reactors were kept under quiescent conditions except during pumping events. Raw sewage was collected from a nearby pumping station, while the brewery wastewater was collected from the Yatala Brewery Industry. The reactors were operated for several months to establish pseudo steady-state conditions and to develop mature anaerobic biofilm on the walls of the reactor and the carriers.

The study was divided into two parts: short and long-term dosing studies. In the short-term dosing study, several batch tests were performed on a sewer reactor that has never been exposed to brewery wastewater. In this study, brewery wastewater concentration of 0 to 100% v/v was used while pH was maintained at a constant level. The long-term exposition tests were carried out to the experimental reactor that has been adapted to the brewery wastewater with two different mixing ratios of 10 and 25% v/v. However, in the long-term study the pH of the system was not controlled.

In the short-term test, different proportions (0, 5, 10, 15, 20, 25, 50, and 100%) of brewery wastewater were added into the sewer reactor separately. This was done to have different VFA levels in the system (ranging between 130 and 290 mg COD/L). During the test, pH was initially set up at pH 7 ± 0.2 . The results of the short-term study are presented in Figure 1.

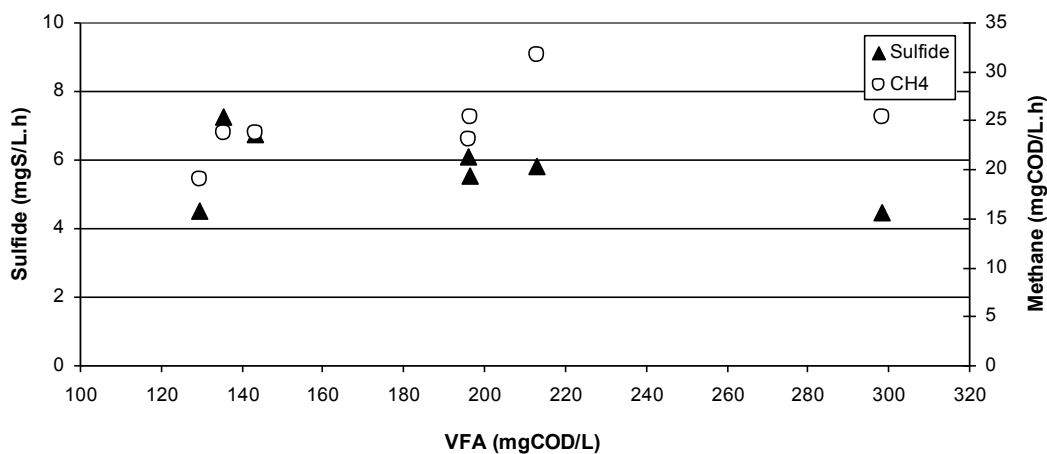


Figure 1. Sulfide and methane production rates during short-term exposition tests

Overall, the addition of brewery wastewater resulted in a higher sulfide production rate compared to the one that did not receive brewery wastewater (control). Since the pH was not the inhibiting factor for SRBs in this case, higher fermentable COD in the system, as the impact of brewery wastewater dosing, has increased the activity of SRBs thereby increasing the sulfide generation rate. However, the general result shows a decreasing trend of the sulfide production rate with further increase in VFA levels. This indicates some inhibiting effects of high VFA. The tests also indicated higher production rates of methane in reactors that were dosed with the brewery wastewater. Availability of fermentable COD at a higher concentration seems to have resulted in a higher methane production rate. However, the production of methane was not inhibited by higher VFA concentration as observed in the case of sulfide generation. Spatial distribution of the SRBs and methanogens (SRB developing near the biofilm surface and methanogens developing in layers deeper in the biofilm) might have resulted in this difference, as the methanogens are not directly exposed to higher VFA concentration as the SRBs.

Overall data for the long-term exposition tests can be depicted from Figure 2 (sulfide production rates) and Figure 3 (methane production rate). Both the figures can be divided into three different periods: Period 1 - baseline study (23rd May-12th Nov 2008), where experimental and control reactors were operated with domestic wastewater; Period 2 - continuous dosing of brewery wastewater at 10% v/v into the experimental reactor (10th Dec 2008-24th Feb 2009); and Period 3 - continuous addition of brewery wastewater at 25% v/v to the experimental reactor (10th March-29th April 2009).

By adding brewery wastewater continuously into the system at 10% v/v, the pH of the sewer system dropped down to 6.6 ± 0.2 with VFA levels of 144.6 ± 63.5 . Under steady state conditions, the sulfide and methane production rates increased up to 40% and 30%, respectively. The lower pH initially resulted in a lower sulfide production rate, but this recovered as the dosing continued. This could be related to the microbial shock load when the new pH level was introduced. However, the microbial community seems to adapt well to the changed pH after 4 weeks of continuous exposition. It is worth mentioning here that the pH varied from 6.6 to about 5.7 during a pumping cycle. This was direct impact of fermentation occurring in the system.

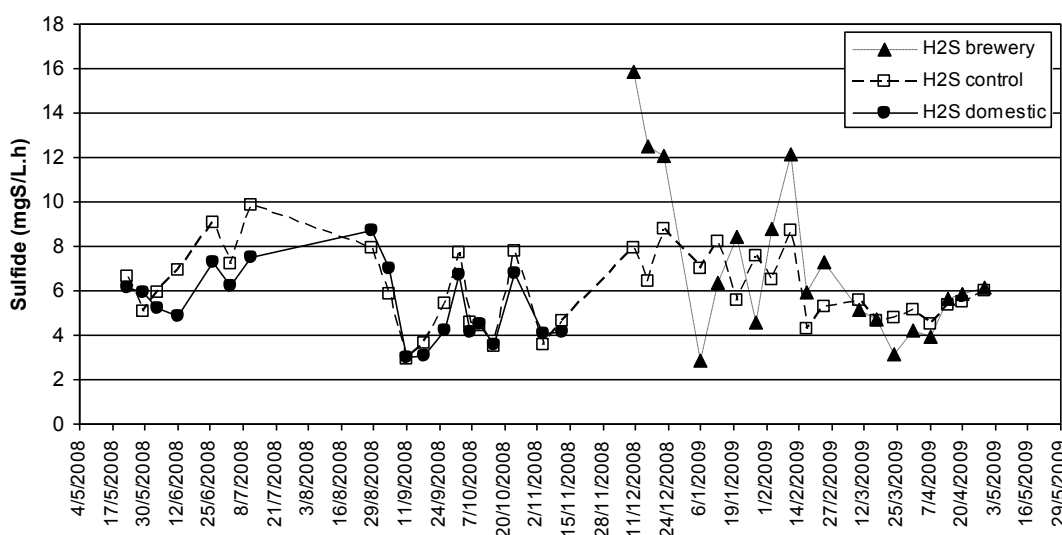


Figure 2. Sulfide production rates during the long-term exposition tests

By increasing the proportion of brewery wastewater to 25% v/v, pH in the reactor was further reduced to 6.2 ± 0.3 with a VFA level of 212.0 ± 34.0 . The sulfide generation rates during the steady state conditions were reduced by 10% as compared to the reference reactor, but the methane generation rate increased by up to 30%. The lower pH seems to reduce the SRB activity in this case. However, the methane production rate was high even at a lower pH. Higher VFA level in the reactor seems to increase the methane production as more VFA is available for methanogenesis. Also, higher COD due to the increase of brewery wastewater proportion results in higher level of fermentation products including hydrogen, which also increases the methanogenic activity. However, in the case of SRB, the impacts of pH seem to have more influence than the increase in VFA as seen by a lower sulfide production rate.

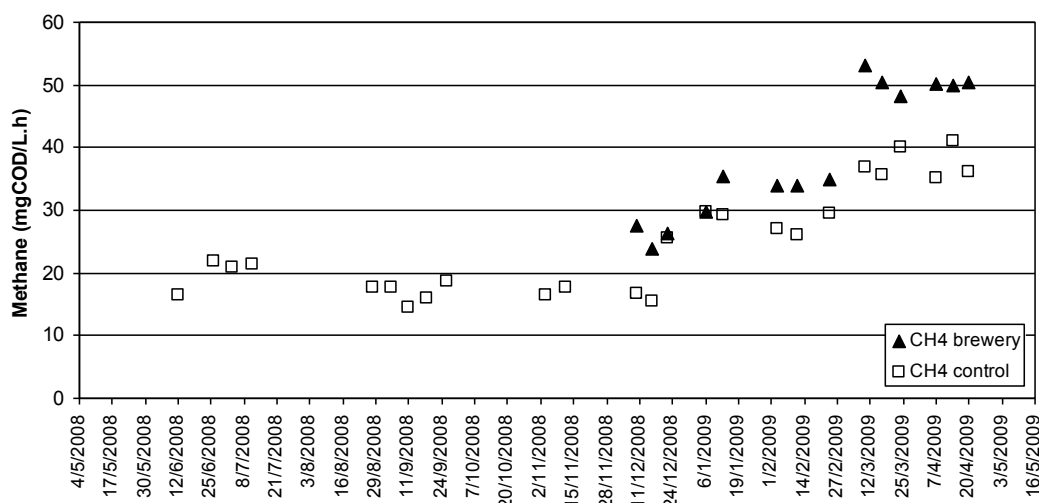


Figure 3. Methane production rates during the long-term exposition tests

The study revealed that the addition of brewery wastewater in general affects the performance of the sewer system with respect to both sulfide and methane production. The introduction of brewery wastewater has two impacts: decrease of pH; and increase in VFA levels. Both of these changes are expected to influence the microbial activity in the system. In the short-term exposition test, introduction of brewery wastewater increased the rates of sulfide and methane production at a constant pH. The sulfide production rate decreased with increased proportion of brewery wastewater, while the methane generation rate increased. In the long-term exposition test with 10% brewery wastewater, higher sulfide and methane production rates as compared to the reference system were observed. When the proportion of brewery wastewater was further increased to 25%, the sulfide generation rate decreased, but opposite was the case with methane production.

3.1.2. DAIRY WASTEWATER

The same reactor system as in the case of brewery wastewater was used. The control reactor was intermittently fed with sewage while the experimental reactor was dosed with a mixture of dairy (10% v/v) and domestic wastewater (90% v/v). In order to characterize dairy wastewater, samples were collected from Parmalat Industry in South Brisbane on three occasion and samples were analysed for various parameters. The wastewater composition varied significantly from batch to batch. To minimize the impacts of the variation of wastewater composition on biofilm activity, synthetic dairy wastewater having a composition that represented average characteristics values was prepared by using skimmed milk powder and other necessary chemicals. The reactors were operated for about 3 months to establish pseudo steady-state conditions and to develop mature anaerobic biofilm on the walls of the reactor and the carriers.

The study was divided into two parts: long and short-term dosing studies. The long-term exposition tests were carried out to the experimental reactor that has been adapted to the dairy wastewater with a mixing ratio of 10 % v/v. However, in the long-term study, the pH of the system was not controlled. A number of batch tests were performed in each stage to observe any changes in the sulfate reduction and methane production capabilities of the biofilm resulting from dairy wastewater addition. As the part of the short-term studies, several batch tests with different concentration of dairy wastewaters were performed on a sewer reactor that has been adapted to 10% v/v dairy wastewater. In this study, dairy

wastewater concentration of 0 to 50% v/v was used while pH was maintained at a constant (normal) level.

The changes in sulfate concentration in 90 minutes (length of a batch test) in the reference and experimental reactors, which also gives amounts of sulfide produced in the two reactors, are compared in Figure 4. The amount of sulfate reduced in experimental reactor was always lower than that in the reference reactor. The variation in the amount of sulfate reduced is related to the variation in feed sulfate concentration.

The rates of dissolved sulfide production with different feed concentrations (domestic WW only in reference reactor and 90% v/v domestic WW + 10% v/v dairy WW in experimental reactor) are compared in Figure 5. Similar performances were observed in both the reactors during the baseline study. However, comparison during the second phase of test shows lower production of sulfide in the experimental reactor as compared to the reference reactor. On average sulfide production rate in experimental reactor was 30% lower than that in the reference reactor. Methane production in two reactors (experimental and reference) with different feed compositions is compared in Figure 6. The addition of dairy WW shows decrease in methane production by about 10%.

The results discussed above clearly show that the addition of dairy WW has negative impacts on both sulfide and methane production. The impacts on sulfide production were more severe on sulfide production than on methane production. In addition to the impacts on methane and sulfide production, introduction of dairy WW has also caused decrease in pH. Initial average pH in the reactor with 100% domestic WW was 6.8, while that with 10% dairy WW decreased initially to 6.2 and further decreased to about 6.0 after 2 weeks of exposition to dairy wastewater.

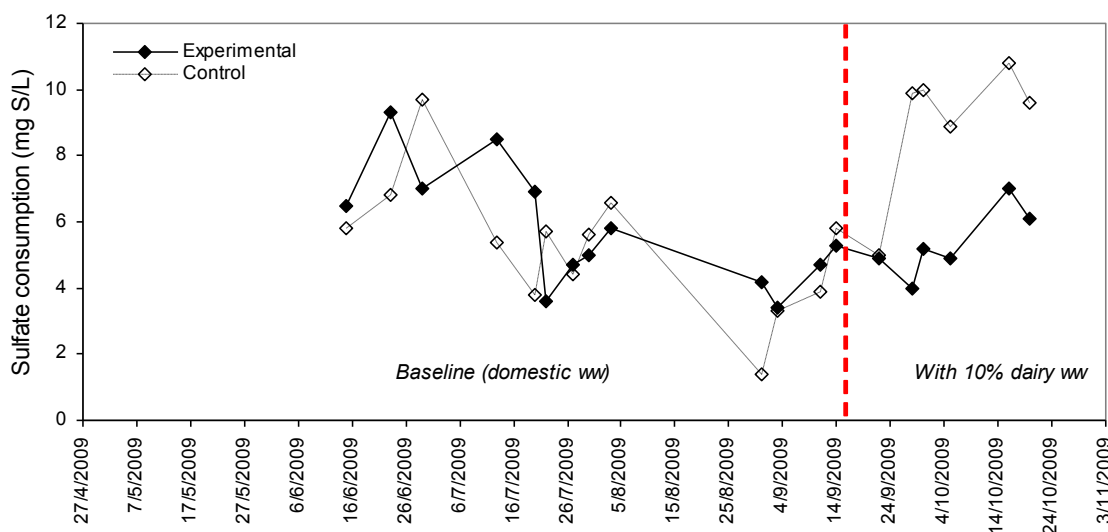


Figure 4. Change of sulfate concentration during the batch tests

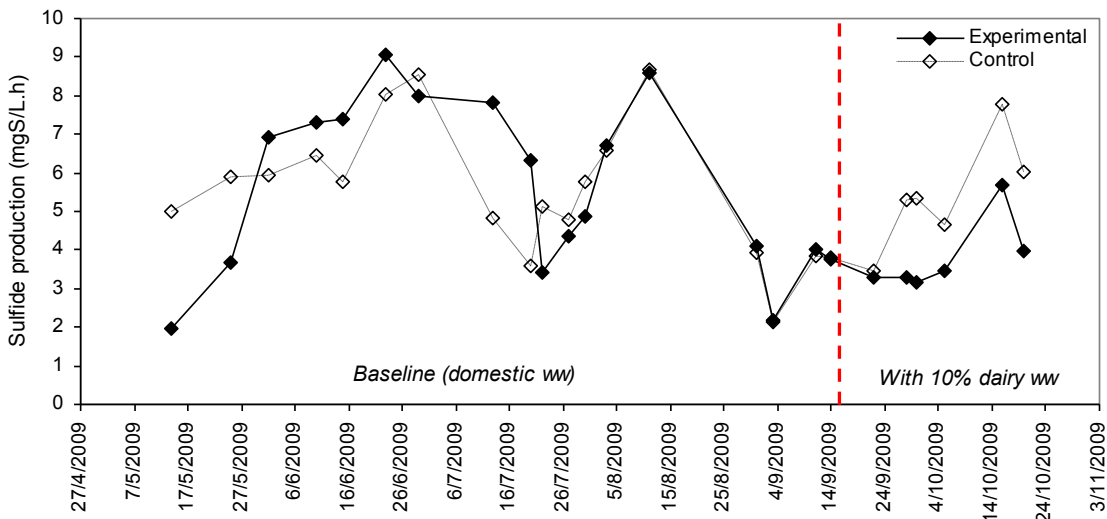


Figure 5. Comparison of sulfide production rate with different feed compositions

The results of the short-term study, where different proportions (0, 5, 10, and 25%) of dairy wastewater were added into the experimental reactor, are presented in Figure 7. The results show that the activity in terms of both sulfide and methane production was highest at 10% addition of dairy WW (corresponding to soluble COD of 630 mg/L). This is mainly because the biofilm was adapted to the similar conditions with respect to sewage composition. Lower activities were observed when the proportion of dairy wastewater was either increased or decreased. At lower soluble COD (sCOD) concentrations, the activity of SRBs and methanogens decreased most likely due to insufficient substrate availability. At higher sCOD concentration, it is likely that the level of unidentified inhibitory compounds increased leading to a decrease of both sulfide and methane rates.

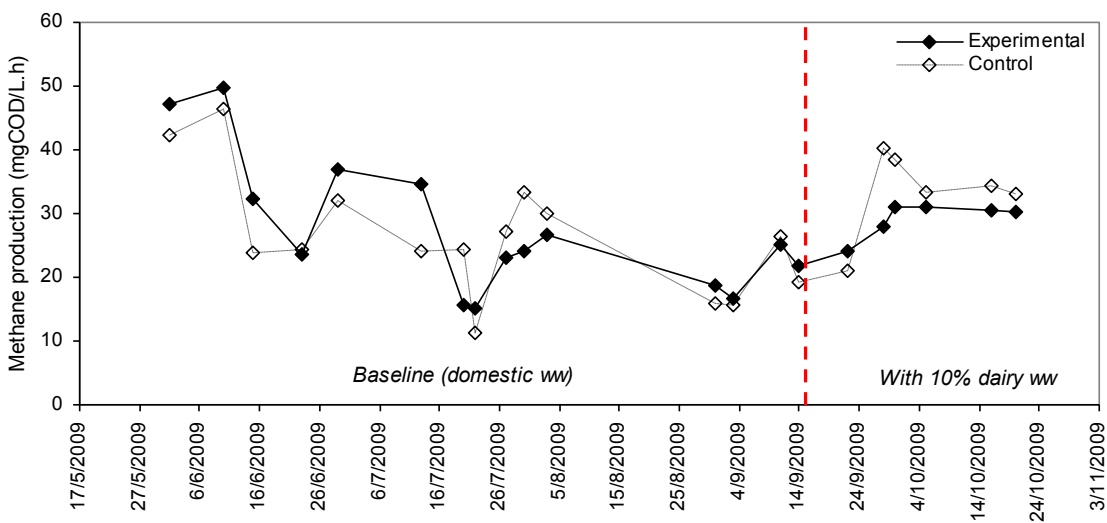


Figure 6. Comparison of methane production

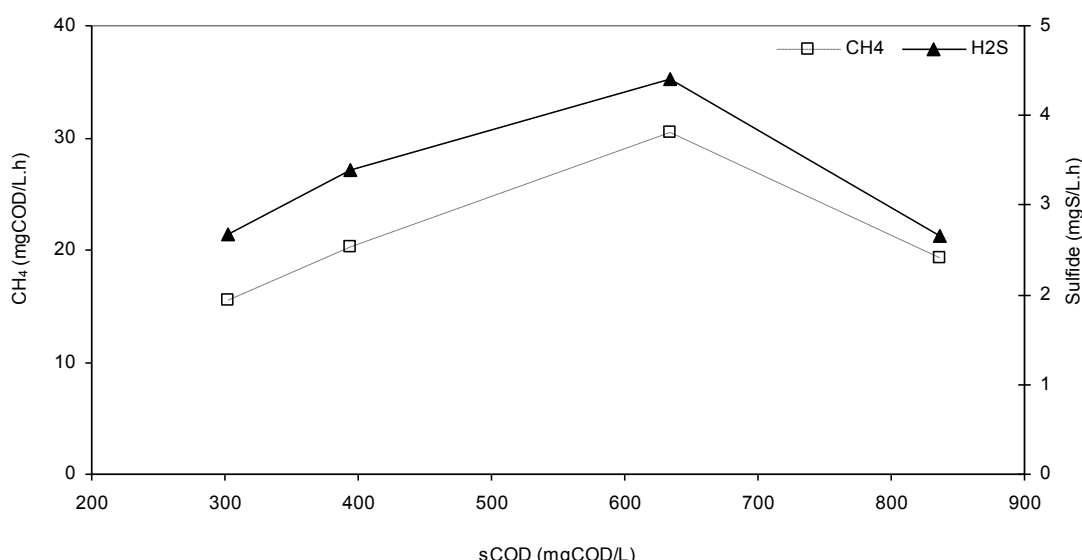


Figure 7. Sulfide and methane production rates during short-term exposition tests

The study revealed that the addition of dairy wastewater affected sulfide and methane generation in a laboratory sewer system. The addition of 10% v/v dairy wastewater resulted in the decrease of sulfide and methane production rates by up to 30% and 10%, respectively. These results are different from those observed with brewery wastewater. No significant change in activity was observed in the latter case despite low pH. A number of postulations are made for the decreased activity and possible causes include: slow biodegradation of dairy waste due to slow hydrolytic step of fat degradation, production of some inhibitory compounds during fat degradation, and absorption of fat to the biofilm surface thereby affecting substrate transfer to the biofilm.

Significant increase in COD concentration and decrease in pH were observed in reactors dosed with dairy WW. The decrease in pH will have significant impacts in a situation where a rising main receiving dairy wastewater discharges into gravity main as liquid-air transfer of H₂S will be higher at a lower pH.

3.2. MODELING OF METHANE PRODUCTION IN SEWERS

The understanding and modelling of methane production in sewers, particularly in rising mains, is essential for its optimal operation as pressured mains are sulfate-rich anaerobic environments where both sulfidogenesis (i.e. sulfate reduction) and methanogenesis (i.e. CO₂ reduction) are similarly favoured from an energetic point of view. The two processes are expected to occur simultaneously using organic materials in wastewaters as electron donors. The synergistic or competitive interactions between methanogenic archaea (MA), sulfate-reducing bacteria (SRB) and fermentative bacteria (FB) are important. However, none of the current sewer models consider methane formation in sewers. This not only results in the inability of these models to predict methane emission from sewers, but also leads to inaccurate predictions of the COD concentration in the wastewater.

This work was conducted to enhance the current sewer models with the capability to predict methane formation in rising main sewers. The model has been calibrated using experimental data obtained from a lab-scale sewer system, and validated using field data. The UQ Sewer Model has been extended to account for the competition between SRB and MA for the common electron donors.

The UQ Sewer Model has been extended to account for methanogenic activity with the processes schematically summarised in Figure 8. In current sewer model, acetate is assumed to be the only fermentation product, in line with the IWA activated sludge model. As H₂, which is produced by fermentation, is an electron donor for methanogens, fermentation in this study is modeled as two separate processes: acetogenesis and acidogenesis. Consequently three fermentation products are considered, namely H₂, acetate and propionate.

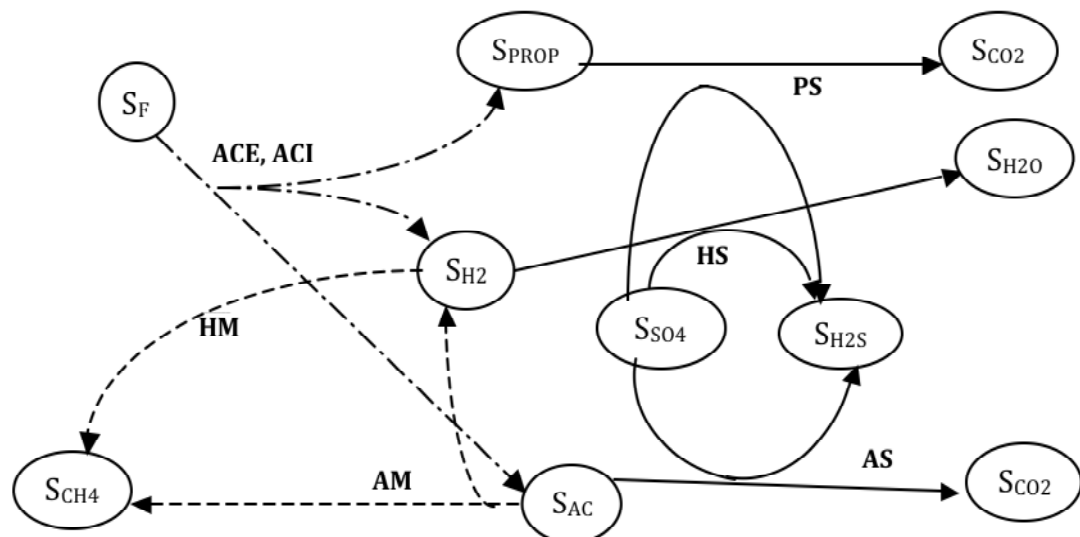


Figure 8. Schematic representation of the model, SRB processes (solid line), FB processes (dash-dotted line) and MA processes (dashed line)

Two data sets with two different reactors (RM2 and RM3) were used in the parameter estimation. The estimated model parameter values are presented in Table 1Table 1, along with the 95% confidence intervals of these estimates. An excellent fit could be achieved between the experimental and simulated profiles for methane, sulfur species and various COD fractions. The model accurately describes the experimental profiles obtained, particularly methane formation which occurs simultaneously with sulfate reduction.

Table 1. Parameter estimation values for the model

	Value	Units		Value	Units
q _{ACETOG}	12.2 ± 0.54	g COD _{GLUC} /m ² -d	K _F	10	g COD/m ³
q _{ACIDOG}	2.14 ± 0.61	g COD _{GLUC} /m ² -d	K _{H2,SRB}	0.01	g COD/m ³
k _{H2S,H2}	< 0.001	g S _{H2S} /m ² -d	K _{AC,SRB}	5	g COD/m ³
k _{H2S,AC}	1.36 ± 0.09	g S _{H2S} /m ² -d	K _{PROP}	5	g COD/m ³
k _{H2S,PROP}	0.90 ± 0.23	g S _{H2S} /m ² -d	K _{SO4}	1.8	g S/m ³
k _{CH4,H2}	1.92 ± 0.29	g COD _{CH4} /m ² -d	K _{AC,MA}	1	g COD/m ³
k _{CH4,AC}	4.44 ± 0.17	g COD _{CH4} /m ² -d	K _{H2,MA}	0.002	g COD/m ³

This model was validated with lab-scale and field data. The lab-scale data used were those measured on a separate sewer reactor (RM1) during normal reactor operation. This reactor received fresh sewage every pumping event (dotted lines). The biological model with the parameter estimates in Table 1 was extended with the hydrodynamic model of the lab reactor system. The experimental and the modeled data are in good agreement (Figure 9), which indicates that the model describes well the biological activities in RM1, despite of the fact that no RM1 data were used in model calibration. The results indicate that both methanogenesis and sulfidogenesis can be reasonably well predicted with the simple conceptual model presented in Figure 8.

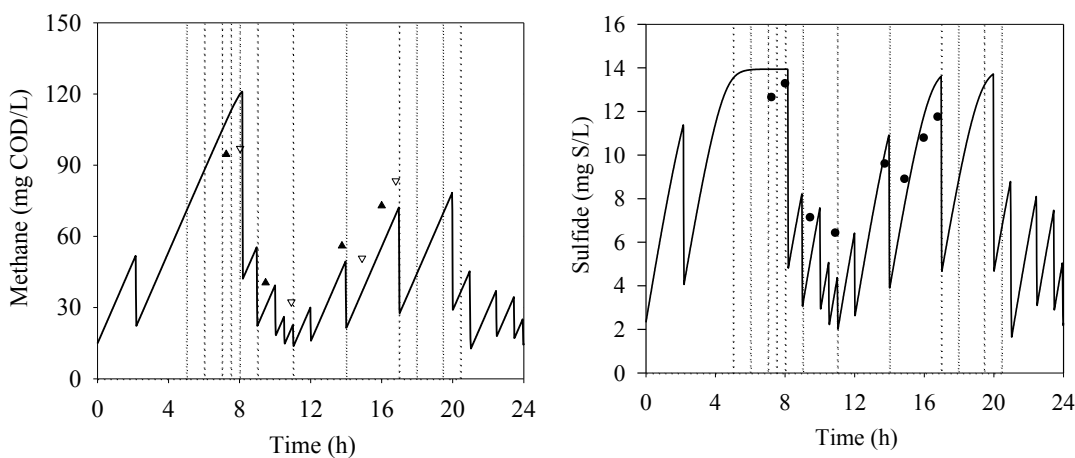


Figure 9. Model validation: experimental (triangles and circles) and modelled (solid lines) profiles of sulfide and methane during a one-day normal operation of RM1. The dashed lines show pumping events.

The model was also validated with the field data measured from the UC09 sewer system of Gold Coast Water (Australia). The variation of flow rate in the UC09 rising main is illustrated in Figure 10(A). The intermittent flow pattern is due to the pump being turned on and off at regular intervals depending up on the volume of wastewater entering the wet well. Methane and sulfide field measurements and model simulation results are compared in Figure 10(B) and Figure 10(C), respectively. The model is able to reproduce the sulfide and methane concentrations reasonably well thereby validating the model.

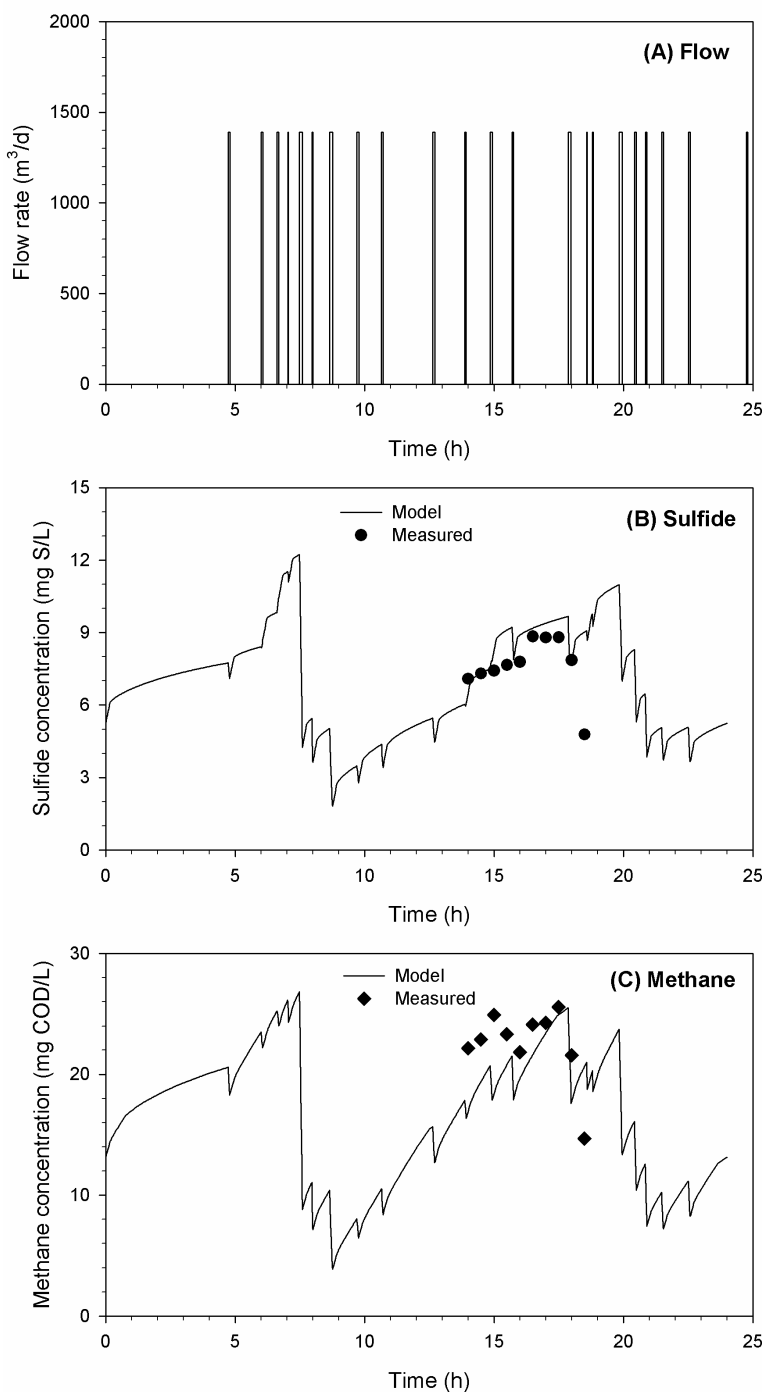


Figure 10. Comparison of modelling predictions for the UC09 rising main with field data obtained from this site (A) Pumping events; (B) sulfide; and (C) methane

3.3. MODELING OF IMPACTS OF pH ON SULFIDE AND METHANE PRODUCTION

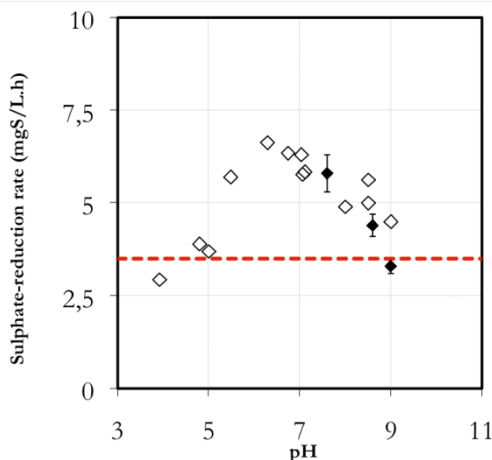
Elevation of pH in sewers by dosing chemicals such as magnesium hydroxide, caustic soda or lime is employed to prevent H_2S release from liquid to gas phase. The pH level directly influences the growth of SRB and MA in sewer systems. SRB grow optimally at pH ranging from 6 to 8, whereas MA prefers pH ranging from 6.5 to 7.2. Outside of these ranges, the SRB/MA development is limited and thus a reduced sulfide/methane production is expected. However, very few experimental data are available suggesting the reduction of the

biological rates induced by pH elevation. Our previous study has shown that a reduction of 30% and 64% of the sulfide production rate for a pH increased from 7.6 to 8.6 and then to 9.0 and a total inhibition of the methane production for similar pH variations. Moreover, uncertainties about the process of inhibition at high pH (direct inhibition by pH or indirect inhibition by free ammonia) are reported. A study was conducted to evaluate the impacts of pH on the rates of sulfide and methane production in anaerobic sewer biofilm, identify the mechanism of inhibition at high pH and develop a model for the impacts of pH on sulfide generation.

The results of the study showed that:

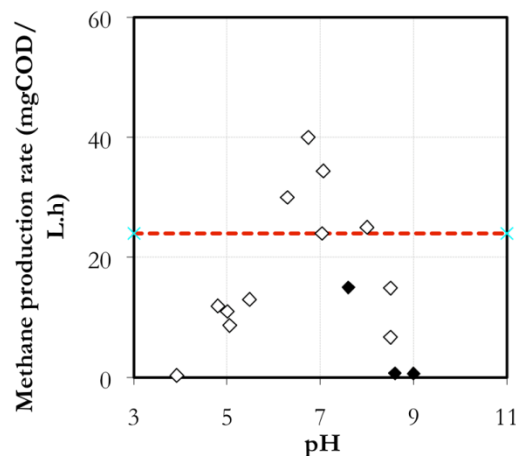
- A maximum sulfate reduction rate of about 7 mg S/L.h was observed at pH 6.5. Any deviation of pH from this level induced a decrease of the sulfate reduction rate. A low sulfate reduction rate of 3.5 mg S/L.h was observed at pH 4.0 and 9.0, which suggests significant inhibition at these pH levels (Figure 11a).

◊ short-term experiments ♦ Gutierrez et al. (2009)



(a) Sulphate reduction rate

◊ short-term experiments ♦ Gutierrez et al. (2009)



(b) Methane production rate

Figure 11. Evolution of (a) the sulfate-reduction rate (mg S/L.h) and (b) the methane production rate (mg COD/L.h) as a function of wastewater pH

- A maximum methane production rate of about 40 mg COD-CH₄/L.h was observed at pH 6.3 (Figure 11b). A slight variation of the pH in either direction induced a significant reduction of the methane production rate. For a similar variation of the pH, the reduction of the methane production was more significant than the variation of the sulfate reduction rate previously observed. Indeed, a reduction of 50% of the methane production was observed when the pH decreased to 5.5 or increased to 8.0. For the same variation of pH, the sulfate reduction rate only reduced by only 25%. A total inhibition of the methane production was observed at pH of 4.0 and 9.0.
- Figure 12 shows the impact of the free ammonia concentration on sulfate reduction rate and methane production rate. A maximum sulfate reduction rate of 6.5 mg S/L.h was observed at free ammonia concentration of lower than 1 mg N/L. This low FA concentration was related to neutral pH and a low total ammonia concentration (50-60 mg N/L). The sulfate reduction rate decreased with the increase in free ammonia concentration as shown in Figure 12. At a free ammonia concentration of 26 mg N/L, the sulfate reduction rate was only 2.5 mg S/L.h. The methane production rate also



decreased with an increase in free ammonia concentration. However, the decrease of the methane production rate was more pronounced when the increase of the FA concentration was achieved by increasing pH. This is true for both the long term and short-term experiments.

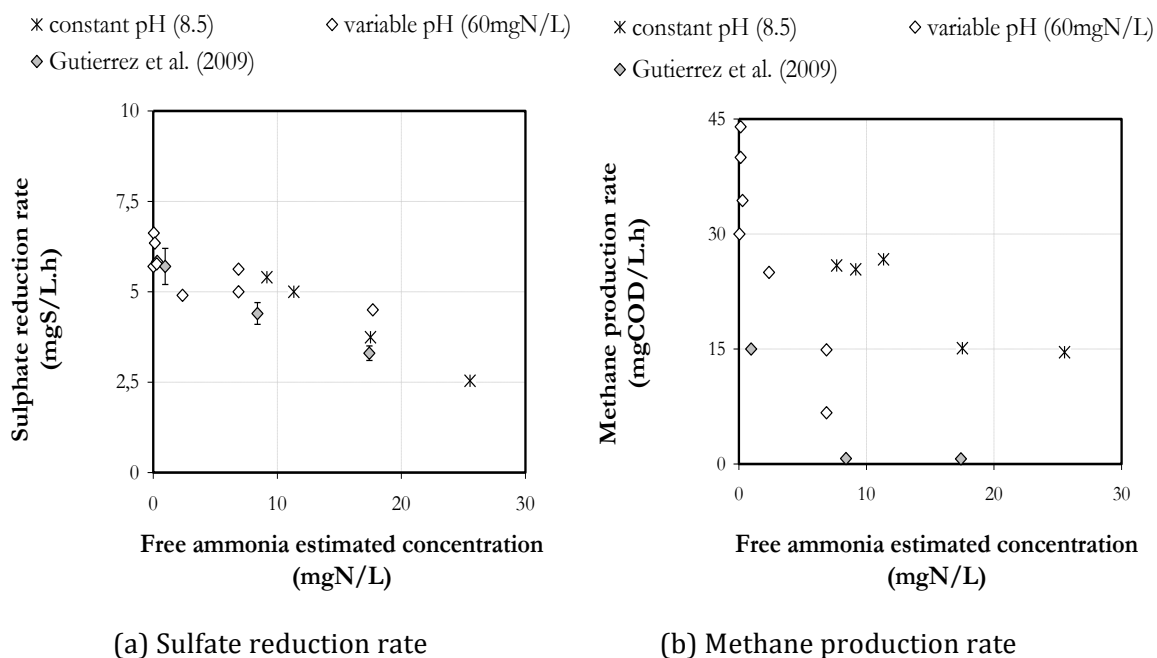


Figure 12. Impact of the free ammonia concentration on the (a) sulfate-reduction rates (mg S/L.h) and on the (b) methane production rate (mg COD/L.h)

- The following model describes the effects of pH on sulfide production:

For $\text{pH} < \text{pH}_{UL}$,

$$k = k_{\max} \cdot e^{\left\{ -3 \left(\frac{\text{pH} - \text{pH}_{UL}}{\text{pH}_{UL} - \text{pH}_{LL}} \right)^2 \right\}} \cdot I$$

For $\text{pH} > \text{pH}_{UL}$,

$$k = k_{\max} \cdot I$$

Where I is the free ammonia inhibition term representing non-competitive inhibition (Siegrist et al, 2002).

$$I = \frac{1}{1 + \left(\frac{S_I}{K_I} \right)^2}$$

Where S_I is the concentration of inhibiting compound (free ammonia in this case) and K_I is the inhibition constant, which is the concentration at which the activity becomes 50% of the maximum activity.

- The following model parameters were obtained by fitting the model to experimental data presented above:

$$k_{\max} = 5.95 \text{ mg S/L-h}$$

$$pH_{UL} = 6.7;$$

$$pH_{LL} = 1.3;$$

$$K_I = 26.15 \text{ mg N/L}$$

Measured sulfide production rate and model predicted rates at different pH levels are compared in Figure 13, while the measured and model predicted rate for different free ammonia concentrations, but at the same pH are shown in Figure 14. As seen from the figures, the model was able to reproduce the measured data very well, thereby validating the proposed model. This model has now been built into the sewer model.

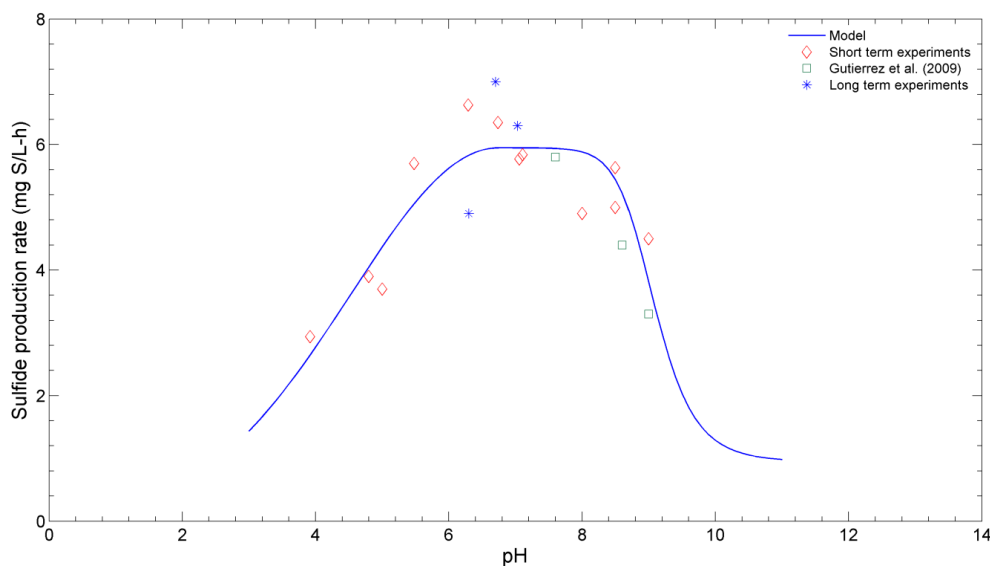


Figure 13. Comparison of measured data and modeling results for pH effect

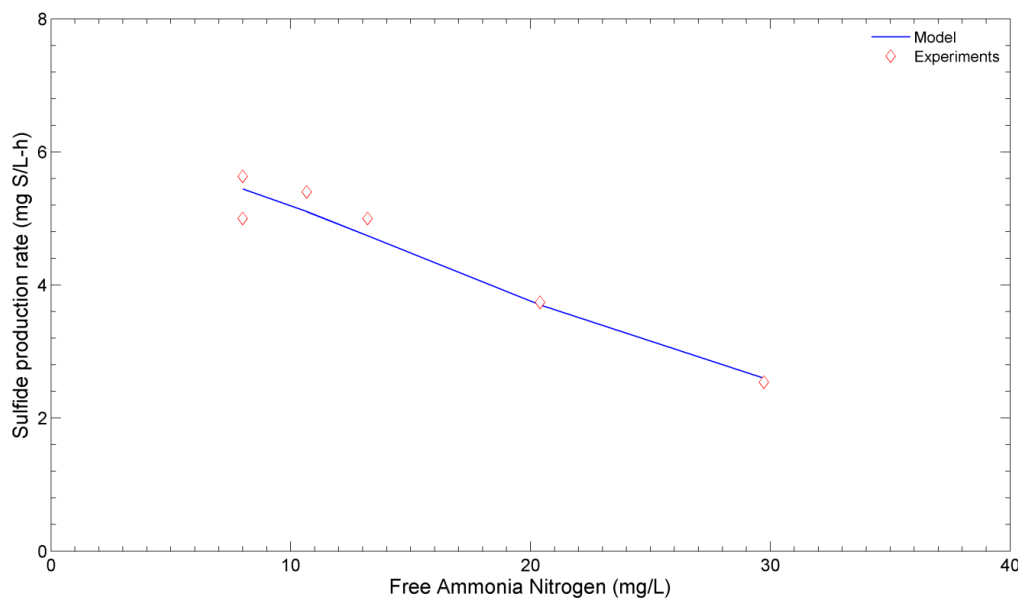


Figure 14. Comparison of measured data and modeling results for free ammonia effect
(Total ammonia nitrogen was varied between 67 to 223 mg N/L, while pH was maintained at 8.5)



3.4. IMPACTS OF FLOW VELOCITY ON SULFIDE PRODUCTION

Sulfide production in sewers is the result of the biological activity in biofilm. The physical and biological properties of the biofilm play an important role in this regard. As the growth and development of biofilm is directly affected by the hydrodynamic conditions it is subjected to, the flow conditions need to be considered in the modelling of sulfide production.

The flow conditions in sewers affect the biofilm in two ways:

- The thickness of the stagnant hydrodynamic boundary layer close to the biofilm-bulk liquid interface, which affects the substrate diffusion into the biofilm, depends upon the flow velocity. Higher the flow rate, the thinner becomes the boundary layer thereby increasing the rate of substrate diffusion into the biofilm.
- Sewer biofilm is subjected to hydraulic shear stress caused by the wastewater flow; higher flow rate resulting in a higher shear stress. The development of the biofilm in terms of its porosity, density and thickness, relates directly to the extent of shear stress it is subjected to.

Two models were setup to investigate the impact of boundary layer thickness on sulfate reduction. A detailed biofilm model in which the biofilm was divided into a number of layers was built, and the biological reactions and diffusion of substrate was modeled in each of these layers. The boundary layer was also divided into a number of layers where only diffusion of substrate was considered.

The model was applied to a batch reactor with a given reactor volume, biofilm thickness and initial substrate concentrations. Simulations were carried out for a number of boundary layer thicknesses and the sulfate concentration profile was plotted in each case (**Error! Reference source not found.**). It was found that the rate of sulfate reduction increased with the decrease in boundary layer thickness until the thickness reached 50 microns. Below this thickness, there was hardly any change in the sulfate reduction rate.

Same biofilm model was employed to a reactor continuously receiving substrate and flow maintaining a constant HRT. Change in the concentration of sulfate in the bulk, in boundary layer and inside the biofilm was evaluated for different boundary layer thicknesses. The results are presented in Figure 16. Increase in the boundary layer thickness resulted in a decrease in the concentration of sulfate at the biofilm surface and hence the reduced sulfide reduction rate. The results show that there is only a marginal change in the profile when the boundary layer thickness is below 50 microns. This suggests that the sulfate reduction rate should not be affected below the boundary layer thickness of 50 microns.

Referring to Figure 17, the boundary layer thickness of 50 microns corresponds to a shear stress of about 0.45 Pa. This implies that the shear stress will have impacts on sulfate reduction only when the shear stress is above 0.45 Pa. Below this level, no impacts on sulfate reduction rate is expected.

In order to validate the above results, a laboratory study was conducted to study the impacts of flow velocity on sulfide generation in sewer biofilm grown on a specific flow condition in a rising main sewer (UC09, Gold Coast). The biofilm samples were collected from UC09 of Gold Coast using a specially prepared detachable pipe section. The pipe section having a diameter same as the rising main in the field (150 mm) was placed along



the UC09 main using detachable joints and biofilm was allowed to grow there under normal sewer conditions for 2-3 months. The pipe section with fully-grown biofilm was detached and then converted to a reactor system using specially designed attachments and accessories (Figure 18). The sewer pipe reactor was designed to have a solid cylinder inside the pipe with a clearance of 15 mm in between the pipe and the inner cylinder. The inner cylinder was connected to an electric motor, the speed of which could be manually adjusted. Changing the speed of the motor could vary shear stress to the biofilm on the wall of the sewer pipe, which depends upon the rotation speed of the inner cylinder and the dimensions of the setup.

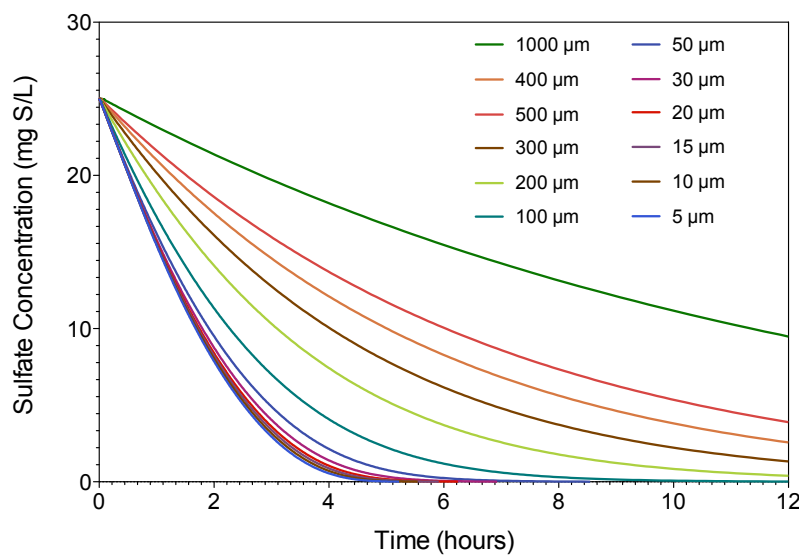


Figure 15. Change in bulk sulfate concentration at different boundary layer thicknesses

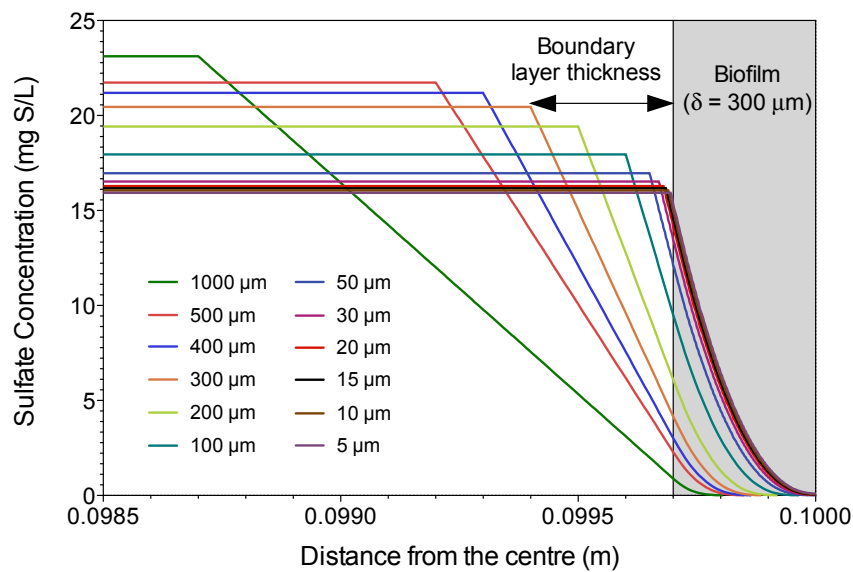


Figure 16. Sulfate concentration profile inside the biofilm for different boundary layer thicknesses

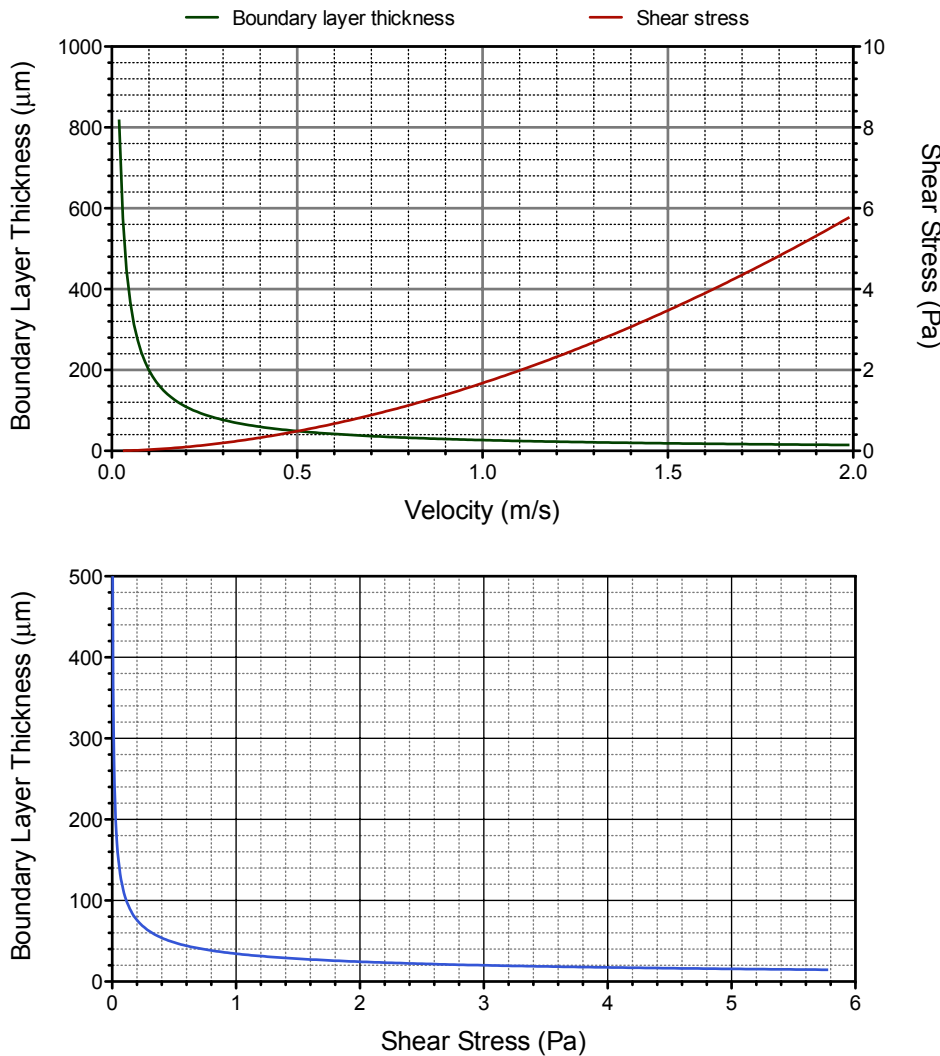


Figure 17. Dependency of concentration boundary layer thickness on shear stress

Three sets of experiments were conducted at different ranges of shear stresses and the results are summarized in Figure 19. As the results show, the sulfate reduction rate increased with the shear stress up to the shear stress of 0.5 Pa. Beyond this, the sulfate reduction rate remained relatively constant. It seems that at a shear stress above 0.5 Pa, full penetration of substrate occurs inside and biofilm, and further increase in shear stress does not have any impacts on substrate diffusion and hence the sulfate reduction rate.

Based on the results of this study, an empirical model to calculate the sulfate reduction rate as a function of the shear stress is developed as follows:

$$k = k_0 + a \cdot (1 - e^{-b\tau})$$

where k is the sulfate reduction rate at a given shear stress (τ), k_0 is the sulfate reduction rate when shear stress is zero, and a and b are the empirical parameters.

The model parameters were estimated by best fit of the data using least square method as follows:

$$k_0 = 3.08 \pm 0.27 \text{ mg S/L-h}, \quad a = 1.54 \pm 0.27 \text{ mg S/L-h}, \quad b = 10.90 \pm 4.88 \text{ 1/Pa}$$

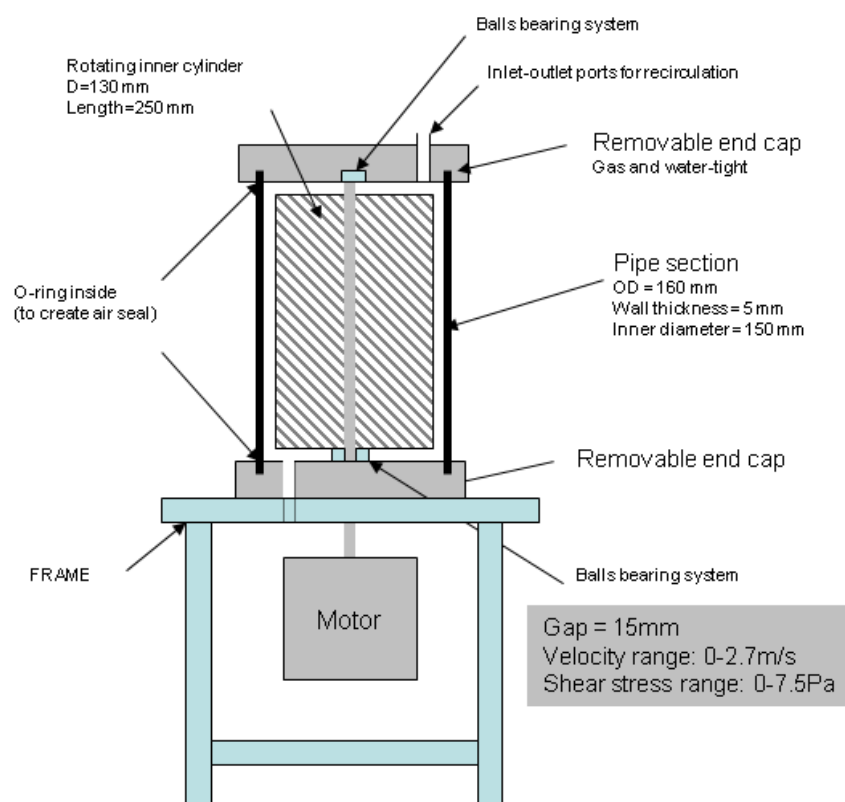


Figure 18. Details of the biofilm reactor

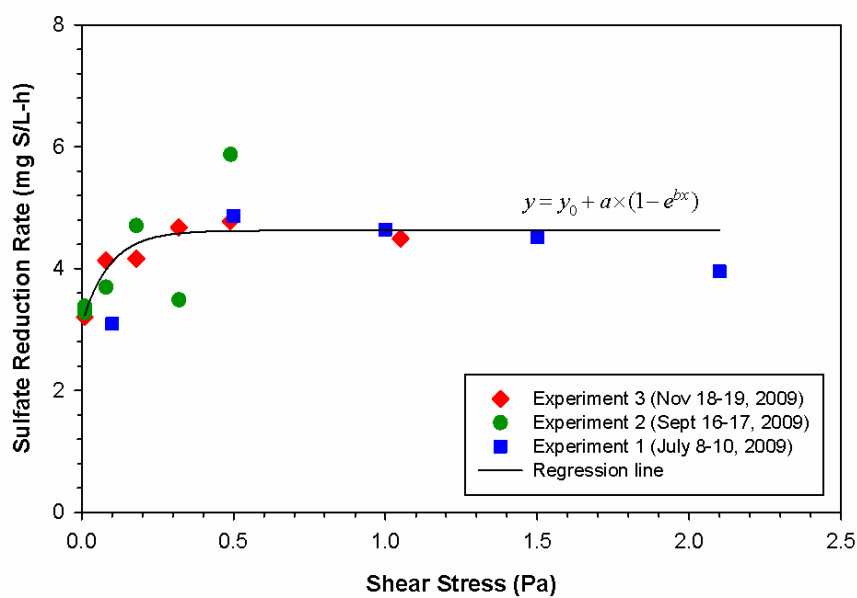


Figure 19. Effects of shear stress on sulfate reduction rate

This model component has been included in the sewer model, and the modification is expected to improve the prediction of sulfide generation in sewers, where significant change in flow rate occurs. It is worth mentioning here that the previous version of sewer model assumes same sulfide production rate irrespective of the flow rate. Differentiation is only made when the flow in the sewer becomes zero.

3.5. EFFECTS OF SEWER SEDIMENTS ON H₂S PRODUCTION

The objective of this study is to determine the effect of sewer sediments on sulfate reduction and methane production in sewers. The study was conducted using six different sediments obtained from Gold Coast, Melbourne, and Sydney. The specific aims of the study were to: (a) determine the maximum sulfate reduction and methane production rates in sewer sediments, (b) investigate the effect of flow velocity thus shear stress on the sulfate reduction and methane production activity of sediments, and (c) determine the sulfate reduction and methane production activity in sewers during stagnant flow conditions. Total of six sediments were collected from three different cities as shown in Table 2.

Table 2. Characteristics of sediments and sampling locations ^a

City	Sediment	Catchment	Sewage Type	Location	Total Solids Content (% wet weight)	Volatile Solids Content (% wet weight)	Bulk Density (g/cm ³)
Sydney	A	Liverpool / Moorebank	Domestic	Pumping Station	79.71 ± 0.59	1.58 ± 0.05	1.66
	B	Moorebank / Wattle Grove	Domestic and industrial	Pumping Station	24.99 ± 3.86	3.73 ± 0.25	1.35
Gold Coast	C	Burleigh Heads	Domestic	Manhole	74.04 ± 0.44	0.71 ± 0.03	2.02
Gold Coast	D	Elanora WWTP	Domestic	Grit Chamber	17.73 ± 0.78	12.08 ± 0.27	1.12
Melbourne	E	Warrandyte, Eltham and Doncaster	Domestic and food industry	Manhole	55.69 ± 3.87	3.38 ± 0.08	1.49
Melbourne	F	Avondale Heights, Keilor, Sunshine North and Tullamarine	Domestic + ?	Manhole	55.50 ± 1.12	5.83 ± 0.34	1.52

^aMean ± standard error (n = 6)

Sediments were analysed for their total and volatile solids content and bulk density. As shown in Table 2, sediments showed quite variability in terms of their total solids (TS) and volatile solids (VS) contents as well as their bulk density. Sediments were collected mostly from pumping stations or manholes. However, Sediment D was collected from a grit chamber of Elanora wastewater treatment plant and therefore, it contains higher VS content compared to others due to the fact that settleable as well as suspended solids are collected via grit chambers. Sediment A, C, and D were collected from locations where only domestic sewage was discharged. Sediments B and E were collected from locations, which received both domestic and industrial sewage. Information of Sediment F is currently not available, however, results suggest that the sediment, which it was collected was also receiving high quantities of industrial discharge.

Sediment B was collected from a sewer, which received wastewater from industries such as food manufacturing, small hospital/laboratory, mechanical workshop, car wash, metal industries, and spray painting. Sediment E was collected from a sewer, which received wastewater from various food industries.

The results of the study showed that:



- Media added serum bottles resulted in lower sulfate reduction and methane production profiles compared to that of the sewage added bottles. Growth media did not contain any carbon source; therefore both the sulfate reduction and methane production were a result of endogenous respiration. Sulfate reduction and methane production rates in media added serum bottles for Sediment A was significantly lower than that of the serum bottles with sewage, suggesting that carbon source contained within the sediment was limiting (Table 3). Sewage added serum bottles showed significant levels of sulfate reduction and methane production for Sediment A. Sediment B showed higher sulfate reduction and methane production activities in the media added serum bottles compared to that of Sediment A (Table 3). Highest sulfate reduction and methane production rates were observed in Sediment C (Table 3). Lowest sulfate reducing activity was observed in Sediment D in spite the fact that it had the highest VS content compared to that of the other sediments. Sediment D was collected from a grit chamber at Elanora wastewater treatment plant, therefore the high VS content could be the result of the content of the settleable and suspended matters that were captured by the grit chamber. Methane production activity was highest in the sewage added serum bottles suggesting that the methanogens were highly active in Sediment D (Table 3).

Table 3. Maximum sulfate reduction and methane production rate of sediments in the absence and presence of carbon source^a

Sediment	Maximum Rate			
	Sulfate reduction <i>k'</i> , g S/m ³ sediment.d [k, g S/kg VS.d]		Methane production <i>k'</i> , g COD/m ³ sediment.d [k, g COD/kg VS.d]	
	Media	Sewage	Media	Sewage
A	2.16 ± 0.38 [0.094 ± 0.018]	50.79 ± 9.54 [2.29 ± 1.04]	2.24 ± 0.16 [0.098 ± 0.021]	48.82 ± 4.28 [2.13 ± 0.36]
B	4.46 ± 0.08 [0.097 ± 0.011]	83.04 ± 4.39 [1.46 ± 0.51]	36.04 ± 14.12 [0.814 ± 0.349]	120.12 ± 30.32 [1.99 ± 0.58]
C	67.04 ± 7.69 [4.57 ± 0.44]	210.47 ± 3.96 [14.43 ± 2.13]	77.60 ± 6.80 [5.27 ± 0.17]	93.79 ± 11.55 [5.27 ± 0.17]
D	0.285 ± 0.048 [0.052 ± 0.018]	0.341 ± 0.22 [0.062 ± 0.04]	31.26 ± 11.09 [0.22 ± 0.06]	139.00 ± 25.64 [0.98 ± 0.18]

^a Mean ± standard error ($n \geq 3$)

- The increase in the mixing speed (and thus flow velocity) resulted in increase in sulfate and methane production rates of Sediments B and C (Figure 20). Methane production rate increased with increased mixing speed in Sediment D, however sulfate reduction did not follow a pattern. Sediment D has shown a very low sulfate reducing activity in both media and sewage added serum bottle experiments, therefore the sulfate reduction rate was very low in reactor experiment as well. Sulfate reduction and methane production rates did not reach to maximum levels, mostly because sulfate only penetrated into first 1-2 mm of the sediment. In addition, methane production rate did not also reach to maximum levels because presumably diffusion of produced methane into bulk liquid was the limiting step.



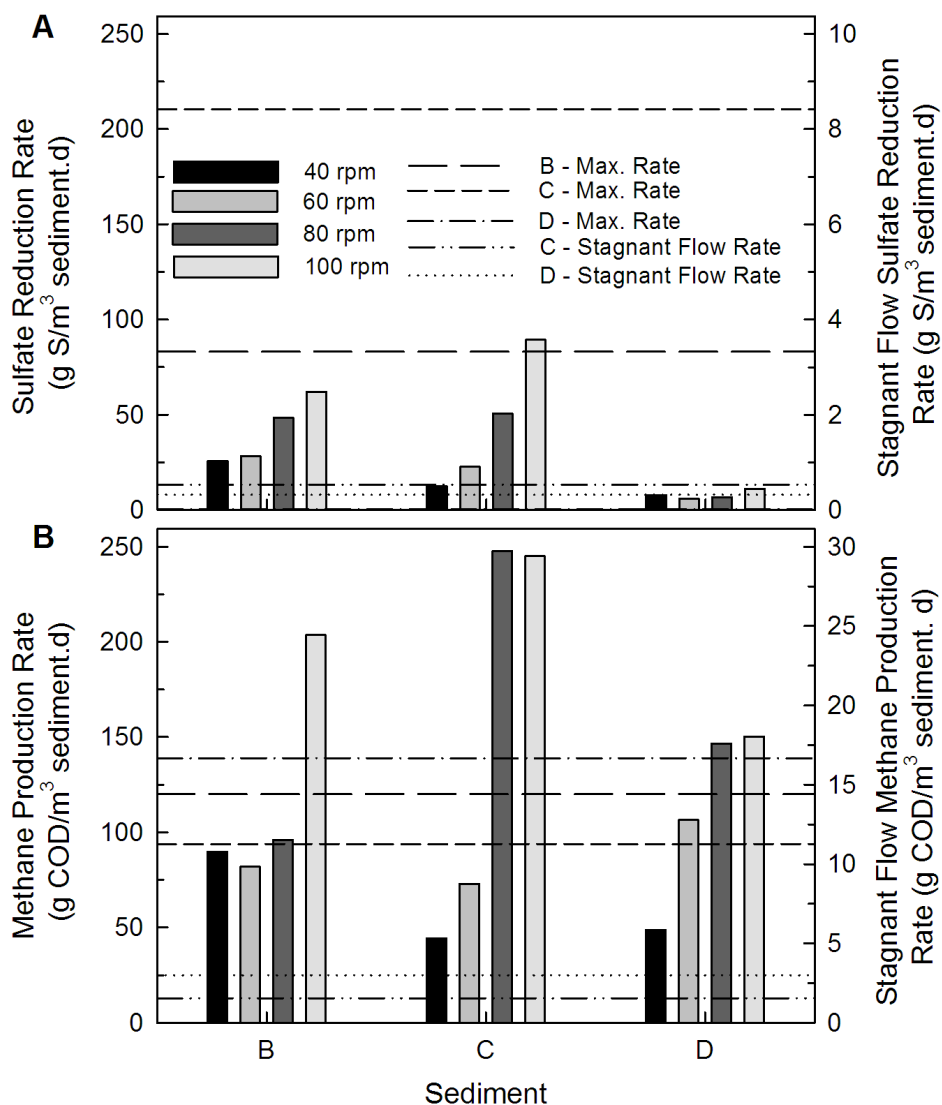


Figure 20. Sulfate reduction (A) and methane production (B) profiles of sediments as a function of stirring speed.

Batch assays investigating the effect of stagnant flow on sulfate reduction and methane production activities of sewer could only be conducted in Sediments C and D. In both sediments both the sulfate reduction and methane production rates were significantly low in both media and sewage added serum bottles (Table 4. Sulfate reduction and methane production in sewer sediments under stagnant flow conditions.

Sediment	Stagnant Flow Diffusion Rate			
	Sulfate reduction		Methane production	
	k^t , g S/m³ sediment.d	[k, g S/kg VS.d]	k^t , g COD/m³ sediment.d	[k, g COD/kg VS.d]
Media				
Sewage				

	0.49 ± 0.19 [0.37 ± 0.28]	0.53 ± 0.14 [0.003 ± 0.001]	1.522 ± 0.351 [1.08 ± 0.26]	1.55 ± 0.142 [1.010 ± 0.001]
D	0.49 ± 0.12 [0.03 ± 0.007]	0.32 ± 0.07 [0.02 ± 0.002]	3.17 ± 1.03 [1.18 ± 0.08]	3.00 ± 0.77 [0.22 ± 0.07]

). Similar results obtained in both the media and sewage added serum bottles suggests that sulfate reduction and methane production processes were not limited by the carbon source but diffusion was the main bottleneck for both processes.

The following conclusions can be made from the results discussed above.

1. Sediments show variable characteristics as a function of the sewer location and wastewater composition.
2. Sulfate reduction and methane production processes under stagnant flow conditions are diffusion limited and these have little contribution to over sulfide and methane production in sewers.
3. Sulfate reduction process is an areal process and thus water flow velocity affects the rate.
4. Methane production is a volumetric process and both exogenous and endogenous soluble carbon sources can be utilized and converted to methane. Flow velocity does not affect the methane production rate.
5. Contributions of the sediments to overall sulfate reduction and methane production in sewers are significant and comparable to that of biofilm processes.

Table 4. Sulfate reduction and methane production in sewer sediments under stagnant flow conditions.

Sediment	Stagnant Flow Diffusion Rate			
	Sulfate reduction		Methane production	
	k^t , g S/m ³ sediment.d [k, g S/kg VS.d]	k^t , g COD/m ³ sediment.d [k, g COD/kg VS.d]	Media	Sewage
C	0.49 ± 0.19 [0.37 ± 0.28]	0.53 ± 0.14 [0.003 ± 0.001]	1.522 ± 0.351 [1.08 ± 0.26]	1.55 ± 0.142 [1.010 ± 0.001]
	0.49 ± 0.12 [0.03 ± 0.007]	0.32 ± 0.07 [0.02 ± 0.002]	3.17 ± 1.03 [1.18 ± 0.08]	3.00 ± 0.77 [0.22 ± 0.07]

A mathematical model that takes into account the diffusion in both bulk phase and in sediments and biological reactions in the sediments was developed. For the modelling purpose, the sediment was assumed to be a homogenous mass with the same sulfate



reduction and methane production activity throughout the depth. Both the liquid boundary and sediment layers were divided into a number of small sections to discretize the layers in space. Following observations can be made from the results of the modeling.

1. The sediment is only partially penetrated with both sulfate and COD, substrates for sulfate reduction and methane production, respectively.
2. Due to relatively high bulk concentration of COD as compared to sulfate, the penetration depth of COD is much higher. This implies that the sulfate reduction occurs only at the top layer of sediment, while the methane production occurs throughout the depth of the sediment. At layers where exogenous COD is not available, methane production using endogenous COD source still continues, although at a reduced rate.
3. Under poor mixing conditions (low velocity in sewers), the build up of the liquid boundary layer results in a much lower substrate concentration at the sediment surface, the extent of reduction being a function of the boundary layer thickness. This further reduces the depth of the penetration of the substrate, and hence the rate of biological reaction using these substrates.

Figure 21 shows the effects of bulk sulfate concentration on sulfide production in sediments. As the figure shows, sulfide production rate increased with the increase in bulk sulfate concentration. Higher bulk sulfate concentration results in an increase in the depth of sulfate penetration in the sediment, making a larger depth of sediment active and hence increasing the overall sulfide production.

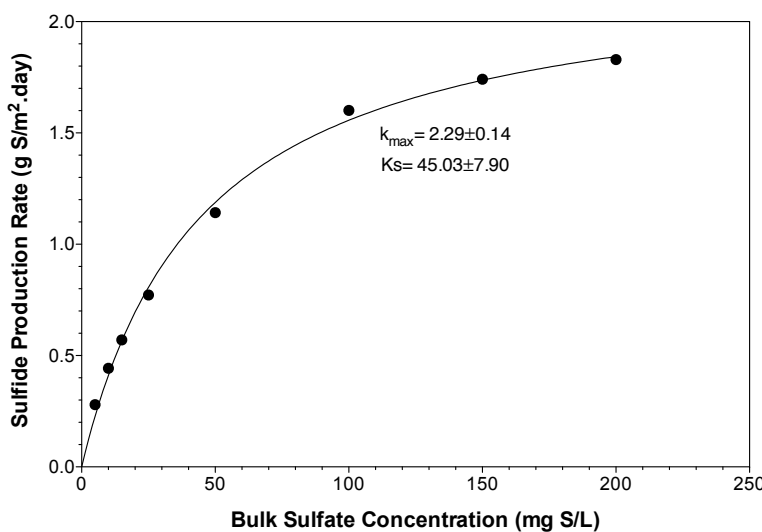


Figure 21. Effect of bulk sulfate concentration on sulfide production in sediments (modeling results)

The dependency of sulfide production rate on bulk sulfate concentration in Figure 21 could be described using Monod type expression as shown below:

$$r_{H_2S} = k_{\max} \cdot \frac{S_{SO_4}}{K_s + S_{SO_4}}$$

Please note that, the COD is assumed to be non-limiting in this case. Parameters in the above model were estimated by curve fitting as illustrated in Figure 21 as follows:



$$k_{\max} = 2.29 \pm 0.14$$

$$K_S = 45.03 \pm 7.90$$

The Monod type relationship can be used to model sulfide production in sewer sediment. Please note that the model parameters should change with the type of sediment, sediment depth and mixing conditions, and hence these need to be calibrated for a given site.

3.6. MODELING OF H₂S TRANSFER IN SEWER PIPES

3.6.1. METHODOLOGY

Experimental work for modelling H₂S transfer in sewer pipes was done using a short section of gravity pipe with flow recirculation. The inlet and outlet chambers were specially designed to minimize the turbulence. Schematic of the laboratory reactor used for this purpose is shown in Figure 22. A photograph of the same system is presented in Figure 23. The laboratory gravity sewer system was operated under a number of conditions with respect to flow rate and the pipe slope. Clean tap water was fed to the setup and circulated continuously using a centrifugal pump. Sodium sulfite was added to the water at the start of each experiment to reduce the dissolve oxygen (DO) concentration to about 1.0 mg/L. Once the water reached this level, continuous measurement of DO commenced.

A model was setup in MATLAB for the experimental setup taking into account the transfer of oxygen to water (aeration) in pipe section, and the dilution of the flow in inlet and outlet tanks, and the recirculation pipe section. It was assumed that no oxygen transfer took place in the inlet and outlet tanks and the recirculation pipe section. The model was then used to estimate the K_{La} value for oxygen transfer by fitting the measured data with the model predictions. K_{La} value was estimated for each set of the operating conditions.

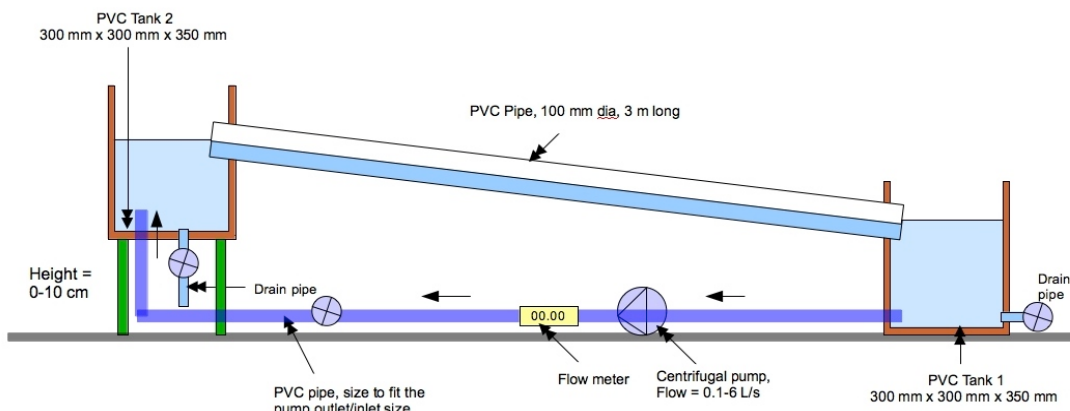


Figure 22. Schematic of the experimental set-up



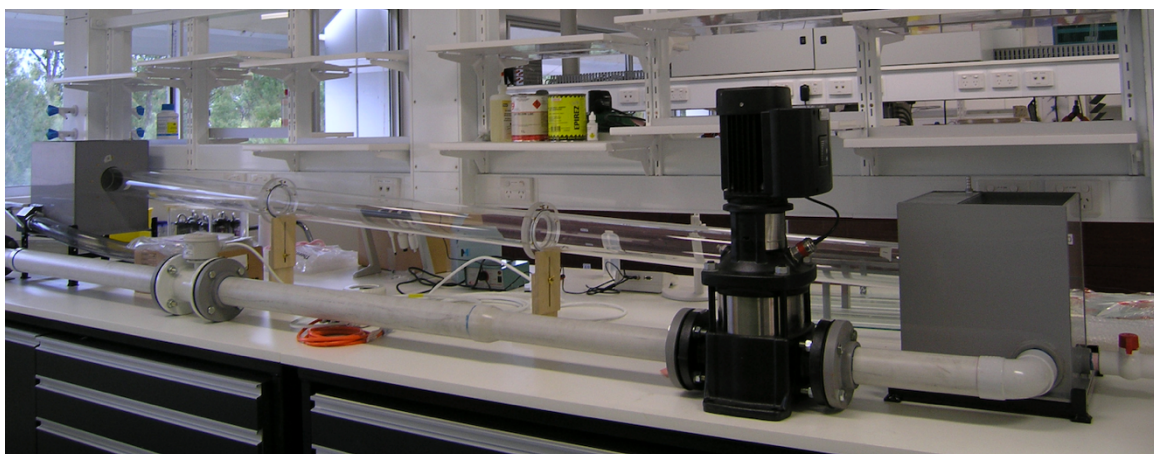


Figure 23. Photograph of the reactor system in the laboratory

Table 5. Summary of experimental conditions (100 mm dia pipe)

S. N.	Slope	Q (L/s)
1	0.025	0.2, 0.3
2	0.020	0.2, 0.3, 0.4, 0.5, 0.6, 1.0, 1.4, 1.7
3	0.015	0.3, 0.4
4	0.009	0.2, 0.6, 1.0, 1.4, 1.7
5	0.0035	0.2, 0.6, 1.0, 1.4, 1.7
4	0.002	0.2, 0.6, 1.0, 1.4, 1.7

Table 6. Summary of experimental conditions for the additional study (200 mm dia pipe)

S. N.	Slope	Q (L/s)
1	0.020	0.2, 0.6, 1.0, 1.4
2	0.009	0.2, 0.6, 1.0, 1.4
3	0.0035	0.2, 0.6, 1.0, 1.4
4	0.002	0.2, 0.6, 1.0, 1.4

Separate tests were conducted by replacing the tap water with sewage disinfected with a hospital grade benzalkonium chloride (1.5%) solution (5.5 mL added to 2.5 L of sewage). Various methods of preventing biological activity of the solids in the sewage were examined and this was found to be the most effective method as the other methods such as chlorine disinfection and autoclaved wastewater did not serve the purpose. Chlorine disinfection did not control the activity and autoclaving apparently changed the composition of wastewater showing unreasonable oxygen consumption behavior. Two sets of tests were conducted for two pipe sizes, 100 mm dia and 200 mm dia.

3.6.2. RESULTS

K_{La} values for the two cases were calculated using the model described above. It was found that the K_{La} value for the sewage was 75% of that for the clean water. The K_{La} values obtained for clean water under different operating conditions were therefore modified using this correlation to obtain the K_{La} values for sewage. K_{La} values were also calculated using the models listed in Table 7 for each set of the operating conditions. The correlation between the measured and model K_{La} values varied from model to model. The predictions were reasonably close to the measured values for K_{La} below 15. Beyond this, the measured K_{La} was generally lower than the model predicted K_{La} .

Table 7. List of current models for the calculation of $k_L a$ for oxygen transfer

S. N.	Model	Expression for $k_L a$
1	Huisman et al(2004)	$k_L a = \frac{1500}{24} \times \frac{\tau \times Re^{-\frac{1}{4}} Sc^{-\frac{1}{2}} (1 + 0.5 \times Fr)}{d_m}$
2	Lahav et al (2006)	$k_L a = \frac{4.842 \times 10 - 7 \times 3600 \times \sqrt{\frac{\rho \times 9.81 \times s \times v}{\mu}}}{d_m}$
3	Krenkel and Orlob (1962)	$k_L a = 7.235 \times (s \times v)^{0.408} \times d_m^{(-2/3)}$
4	Parkhurst and Pomeroy (1972)	$k_L a = \frac{0.96 \times (1 + 0.17 \times Fr^2) \times (s \times v)^{\frac{3}{8}}}{d_m}$
5	Tsivoslou and Neal (1976)	$k_L a = 720 \times s \times v$
6	Taghizadeh-Nasser (1986)	$k_L a = \frac{0.4 \times v \times \left(\frac{d_m}{R}\right)^{0.613}}{d_m}$
7	Jensen and Hvítved-Jacobsen (1991)	$k_L a = 0.96 \times 3600 \times (1 + 0.17 \times Fr^2) \times (s \times v)^{0.75} \times d_m$
8	Jensen (1995)	$k_L a = \frac{0.86 \times (1 + 0.20 \times Fr^2) \times (s \times v)^{\frac{3}{8}}}{d_m}$
9	Balmer and Tagizadeh-Nasser (1995)	$k_L a = \frac{3.82 \times (s \times v \times 9.81)^{\frac{3}{8}} \times d_m^{0.40}}{d_m}$

In order to improve the correlation, the parameters for each of the tested models were optimized collectively for the two experimental data sets by minimizing the sum of the square of errors (predicted K_{La} -measured K_{La}). Out of the 9 models tested here, Models 3, 6, and 9 gave best results in terms of the fit of the measured data. Comparing the SSE among the 9 models, Krenkel and Orlob (1962), Taghizadeh-Nasser (1986) and Balmer and Tagizadeh-Nasser (1995) with modified parameters gave two lowest SSE and hence these models are recommended for calculating the H_2S transfer in gravity sewer.

$$\text{Krenkel and Orlob (1962): } k_L a = 1.98 \times (s \times v)^{0.139} \times d_m^{(-2/3)}$$



$$\text{Taghizadeh-Nasser (1986): } k_L a = \frac{0.39 \times v \times \left(\frac{d_m}{R} \right)^{0.878}}{d_m}$$

$$\text{Balmer and Tagizadeh-Nasser (1995): } k_L a = \frac{10.60 \times (s \times v \times 9.81)^{\frac{3}{8}} \times d_m^{0.646}}{d_m}$$

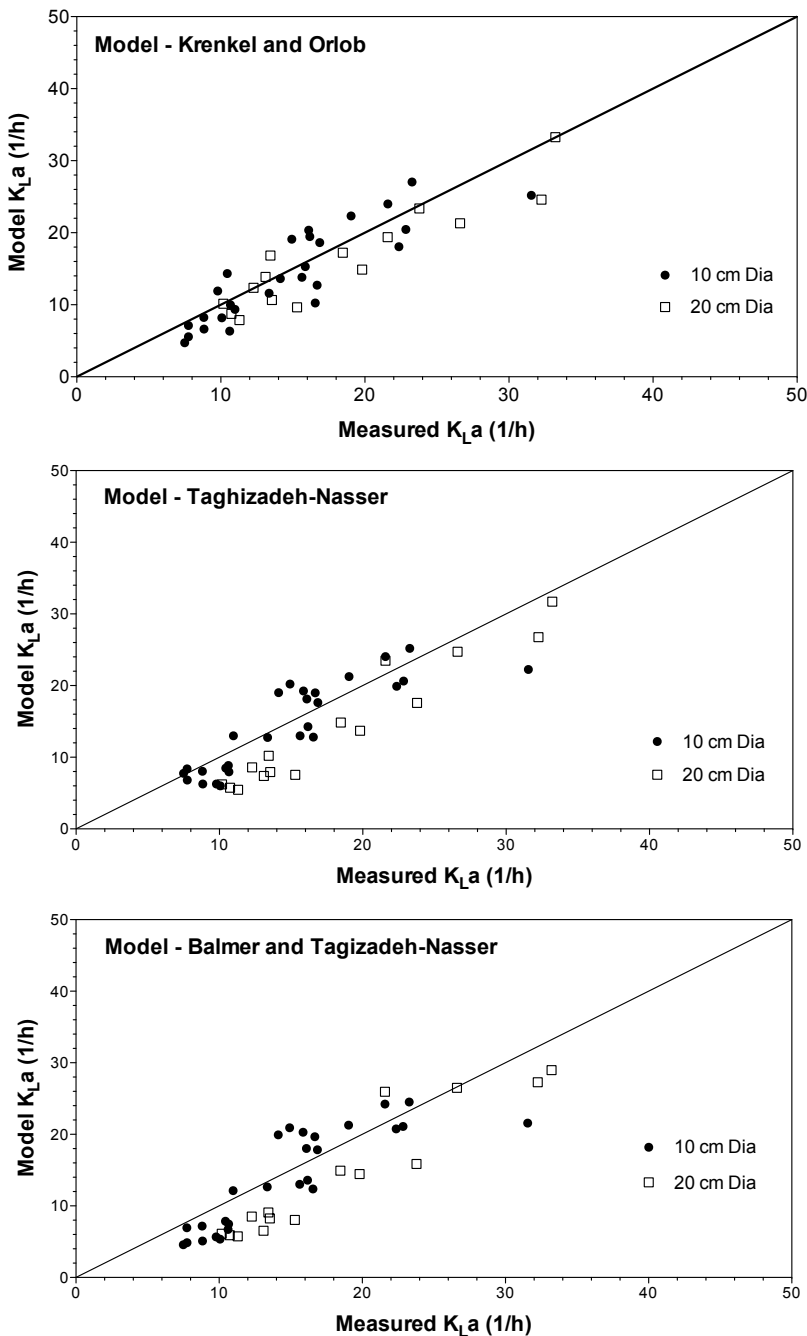


Figure 24. Comparison of the measured and model predicted K_{La} values after parameter optimization

In order to shed some lights on the effects of pipe size, flow rate and the slope (parameters varied in this study), the model results were analysed further. For the given pipe diameter and flow rate, the K_{La} value increased with increasing slope. The extent of the increase in K_{La} was higher for a larger diameter pipe for the same increase in the slope. For the same flow rate and the slope, the K_{La} for a larger diameter pipe was higher than that for a smaller diameter pipe, which is due to large flow width and shallow water depth in the former case. For the same slope and pipe diameter, the K_{La} value was found to depend upon the flow rate. However, the dependency was different for different pipe sizes. For the 10 cm diameter pipe, the K_{La} value decreased with the increase in the flow rate, while for the 20 cm diameter pipe, the K_{La} value increased up to the flow rate of 0.7 L/s, and decreased beyond this flow rate. The dependency is expected to change with the pipe slope. The contrasting trend of the K_{La} value for the two pipe sizes is likely related to the non-linear relationship between the flow rate and the hydraulic parameters affecting the K_{La} value.

3.7. MODELING OF H₂S TRANSFER IN CRITICAL STRUCTURES

3.7.1. BACKGROUND

Several structures are constructed in sewers due to specific hydraulic requirements and these are normally referred as special structures. Their design is based upon the hydraulic requirement. These structures differ in design to suit the conditions that these are built for. The consideration of H₂S emission in general is a much lower priority. However, due to high turbulence created at majority of them, these structures are critically important as the turbulence has a major influence on the release of H₂S gas to atmosphere. Some of these structures are listed below:

1. Inverted siphons
2. Sewer junctions
3. Drop structures
4. Sewer overflow structures
5. Discharge manholes

From the sewer modelling point of view, an accurate knowledge of the extent of H₂S release at these structures is critically important to model the gas phase H₂S concentration in sewers and estimate the H₂S concentration at the exit of the vent pipes installed at these structures.

Since the H₂S emission in the above structures is significantly higher than that in normal gravity sewers, these structures need careful consideration in the model. Different structures affect the transfer differently and hence these need to be dealt with differently.

3.7.2. INVERTED SIPHONS

Inverted siphons behave as a short section of pressure main connecting the up-stream and down-stream gravity pipes, and hence can be modelled as a rising main sections. However, there will be turbulence created at the inlet and outlet. In order to take into account this, two short pipe sections with higher mass transfer coefficient (K_{La}) will have to be included in the model. The proposed approach is illustrated in Figure 25.



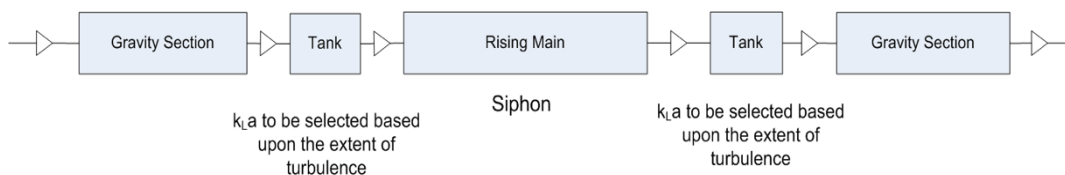


Figure 25. Treatment of inverted siphon in sewer model

3.7.3. DROP STRUCTURES

A model for the drop structure, which takes into account the transfer of gases into and out of the sewage, as described in previous section will be developed. Due to the presence of oxygen, the sulfide will be oxidized and hence the oxidation of H_2S will also be included in the model. A tank model that represents the drop structure needs to be placed in between the two pipe sections (Figure 26). The input data for the drop structure would be the flow entering from the upstream pipe section, depth of water in the tank, and the height of the drop.

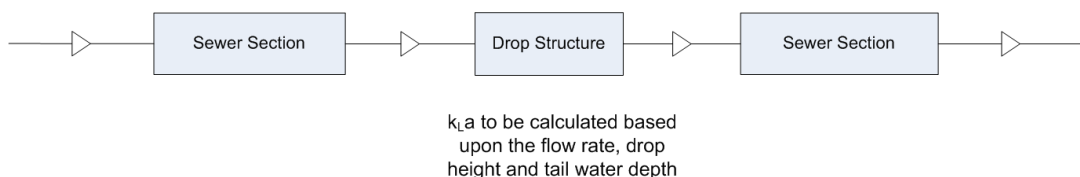


Figure 26. Drop structure in sewer model

3.7.4. DISCHARGE MANHOLES

Discharge manholes at the end of rising main connect the upstream rising main with the downstream gravity sewers. Water level in the discharge manhole rises during pumping in rising main and reaches a maximum level. Once the pump stops, the water level drops to a normal level due to its continuous flow into gravity sewer. In sealed discharge manholes where vent pipe is provided, the air in the headspace of the manhole is pushed out through it when water level rises (Figure 27). In other cases, the air with high concentration of H_2Sg exits through available openings. Since the rising of water level is associated with high turbulence due to pumping of sewage into the manhole, higher levels of H_2Sg are expected. On the other hand, when the water level drops, fresh air is sucked in through the vent pipe or any other openings thereby diluting H_2Sg already in the headspace. This phenomenon results in continuous spikes of H_2S concentration in the gas phase.



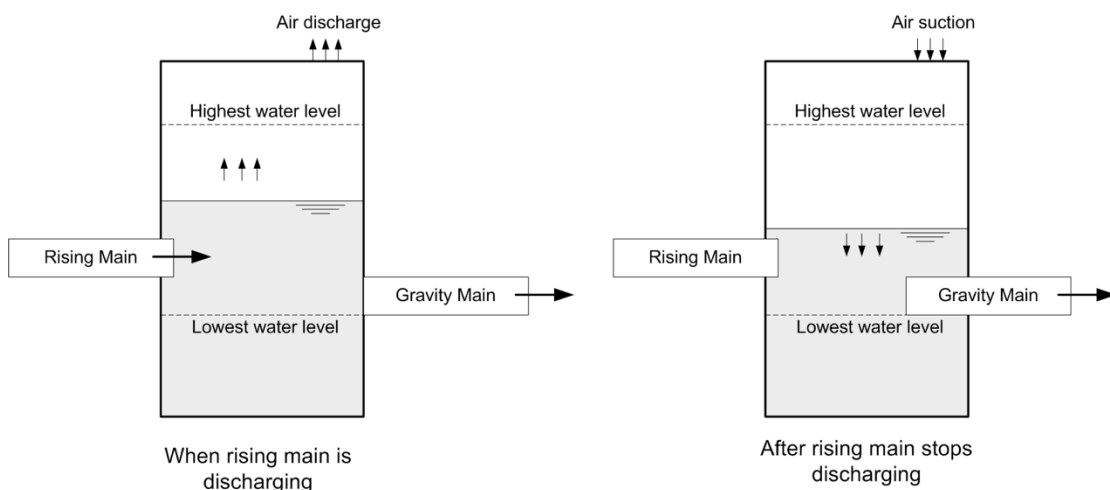


Figure 27. Illustration of the operation of discharge manhole

A model for discharge manhole therefore needs to consider the transfer of gases, change in headspace volume and resulting dilution effect and oxidation of sulfide. The gas-liquid mass transfer coefficient (K_{La}) for H_2S transfer should be considered to increase significantly during the pumping event as higher turbulence is expected.

3.7.5. OTHER STRUCTURES

A tank model, which includes the liquid-gas transfer model and the sulfide oxidation model, needs to be placed in between the two pipe sections (Figure 28). A reasonable K_{La} value needs to be assigned to the transfer model depending upon the extent of turbulence.

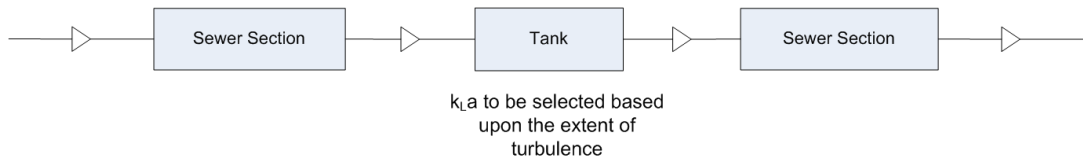


Figure 28. Illustration of the inclusion of special structures in sewer model

3.8. MODELING OF H_2S TRANSFER IN DROP STRUCTURE

3.8.1. MODEL DESCRIPTION

A number of factors such as drop height, shape of the drop, flow rate, and tail water depth affect the oxygen transfer in drop structures. The transfer rate together with the drop structure dimensions and the air ventilation rate determine the gas phase H_2S concentration. Mathematical models developed to estimate oxygen transfer in drop structures are available in literature, and field as well as the laboratory studies have verified some of these models. Since the oxygen transfer into the sewage and the H_2S release to atmosphere are driven by a common phenomenon, these results can be employed to estimate the rate of H_2S release by taking into account the relative diffusivities.

A number of options for modelling H_2S transfer in a drop structure were presented in the previous report. After a review of these options, a model adapted from Zytner et al. (1997)



has been proposed for the sewer model. Although, the model is a steady state in nature, this can be made dynamic by calculating K_{La} value for each set of the influencing parameters. The model takes into account all the factors listed above and can predict the dynamic behavior of the H_2S release in the drop structure.

Details of the adapted model are given below.

The oxygen deficit ratio (r_0) at 20°C can be calculated as follows:

$$\ln r_{0,20}^* = 1.048H^{0.765}Q^{-0.140}D^{-0.071}$$

where H is the drop height in m, Q is the flow rate in L/min and D is the tail water depth in m.

The oxygen deficit ratio (r_0) can be normalized for temperature using the following expression:

$$\ln r_0^* = \ln r_{0,20}^* \{1 + 0.0168(T - 20)\}$$

The deficit factor can be corrected for wastewater using the clean water data using the following expression with the value of α being 0.67.

$$r_0 = (r_0^*)^\alpha$$

The deficit factor for H_2S can then be calculated using the following relationship.

$$\gamma = \sqrt{\frac{D_{H_2S}}{D_{O_2}}}$$

$$r_{H_2S} = r_0^\gamma$$

Based upon the H_2S deficit ratio calculated above, saturation H_2S level (C_s), and the known upstream H_2S concentration (C_1), downstream H_2S concentration (C_2) can be calculated as follows.

$$r_{H_2S} = \frac{C_s - C_1}{C_s - C_2}$$

Finally, the volumetric mass transfer coefficient (K_{La}) can be obtained using the following relationship.

$$K_{La} = \frac{C_1 - C_2}{\theta_H (C_2 - C_g / H_c)}$$

where,

θ_H = Hydraulic residence time in tail water (h)

C_g = Mass concentration in gas phase (kg/m³)

H_c = Henry's coefficient (m³ liquid/m³ gas)



The above model for H₂S transfer in a drop structure was implemented in MATLAB and was employed to simulate different scenarios with respect to flow rate, drop height, tail water depth and the ventilation rate. The dimensions of the drop structure were assumed as follows:

Length = 1.0 m

Width = 1.0 m

Total height = 6.0 m

Tail water depth = 0.10 to 1.0 m

Flow rate = 0.25 to 5 m³/h

Drop height = 1.0 to 5.0 m

3.8.2. SIMULATION RESULTS

Mass balances in both the liquid and gas phases of the enclosed drop structure were carried out incorporating the liquid gas mass transfer of H₂S as follows.

Rate of H₂S transfer:

$$r_{H_2S} = K_L a \left(C_{H_2S,aq} - C_{H_2S,sat} \right)$$

Mass balance in the liquid phase:

$$\frac{dC_{H_2S}}{dt} = \frac{Q}{V_W} \left(C_{H_2S,in} - C_{H_2S} \right) - r_{H_2S}$$

Mass balance in the gas phase:

$$\frac{dC_{H_2S,g}}{dt} = r_{H_2S} \cdot \frac{V_W}{V_A} - \frac{Q_V}{V_A} \cdot C_{H_2S,g}$$

Where C is the concentration, Q is the water flow rate, Q_V is the air ventilation rate, V_A is the volume of air and V_W is the volume of water.

The results of the simulation study are presented in Figure 29. There was a small change in the liquid phase sulfide concentration in all the cases. However, the corresponding gas phase H₂S concentrations were considerable, and the impact of the influencing parameters was clearly seen in the gas phase. As it can be seen from the figure, the gas phase H₂S concentration increased with flow rate and drop height. However, the trend was non-linear. The tail water depth showed very little impact on the gas phase H₂S concentration. As expected, an increase in the ventilation rate resulted in decreasing gas phase H₂S concentration. An understanding of the ventilation rate is required for accurate prediction of gas phase H₂S concentration in a drop structure. The above drop structure model can be used to an enclosed drop structure with limited ventilation.

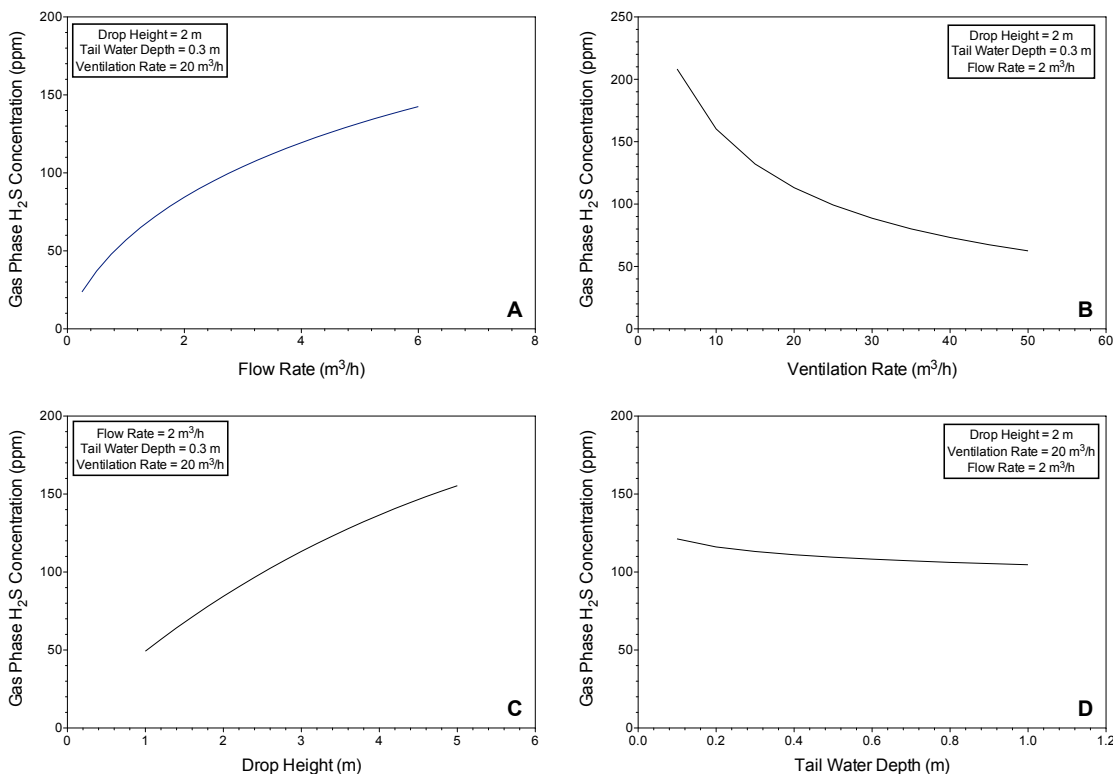


Figure 29. Effect of (A) flow rate, (B) ventilation rate, (C) drop height, and (D) tail water depth on gas phase H₂S concentration in an enclosed drop structure

3.9. FERRIC INHIBITION TO SEWER BIOFILM

3.9.1. BACKGROUND

Bellambi Sewer System of Sydney Water is receiving ferrous dosing for a number of years and a very effective control of sulfide at the WWTP plant has been achieved through the optimisation of the chemical dosing. Ferric dosing to sewer biofilm has shown significant inhibition to sulfide production in a laboratory test. In order to investigate the effects of ferric dosing to the sewer biofilm activity and verify the laboratory findings in the field conditions, a field study was conducted in Bellambi sewer system. The chemical dosing was switched to ferric for several weeks prior to the field study. A number of parameters representing wastewater characteristics were monitored for 6 hours at a number of locations following 4 wastewater slugs and the data thus collected was analysed.

3.9.2. FIELD STUDY

The field study was conducted on 28th of September 2011. The details of the field study are given below:

- Four sampling locations were selected along the length of Bellambi sewer line based upon the discussion with Sydney Water.
 - SP0796 wet well (0 m)
 - Stuart Park (2260 m)



- Towradgi Creek (6490 m)
- Inlet to Wollongong STP (9894 m)
- Historical flow data was collected.
- Four slugs of wastewater leaving the wet well were monitored (at 8:00 am, 9:00 am, 10:00 am and 11:00 am).
- HRT for each of the pipe sections was calculated for each wastewater slugs based upon the historical flow data. Sampling time at each of the sampling location was estimated based on the HRT data.
- Collected samples were analysed for sulphur species, methane, VFAs and total iron. In addition, pH and temperature of each of the collected samples was measured.
- Actual flow data on the day of sampling was obtained and assumed flow used in sampling time calculation and actual flow were compared. While comparing the flow used for the calculation of sampling time for various wastewater slugs and flow measured on the sampling day, it has been found that actual flow rate for Slug 1 was 18% lower than the flow rate assumed, while for other slugs the variation ranged from 2.5% to 8.0%.

3.9.3. RESULTS

The changes in the concentration of sulfate, total dissolved sulfide, VFAs and methane along the length of sewer for each of the 4 wastewater slugs monitored is shown in Figure 30, while the change in pH is shown in Figure 31. The wastewater temperature varied from 16 to 19°C during the sampling.

Some data points are missing as sample could not be collected in one occasion and surprisingly high sulfate concentration was observed in another occasion, which has been ignored in the analysis.

First 2260 m of pipe shows no sulfate reduction (sulfide production) as no change in sulfate concentration is observed. The second section of sewer (2260-6490m) shows production of sulfide as a clear decrease in sulfate concentration is observed. The third section (6490-9894m) shows no sulfate reduction. In fact, some increase in sulfate concentration has been observed.

The rising main sewer studied here discharges wastewater to a discharge manhole from where the wastewater overflows through a weir onto a collection channel. The wastewater is then mixed with other flows before it enters the STP. As the samples at the end of the Bellambi sewer system were collected from the discharge well, there is a possibility that a portion of sulfide might have been oxidised to sulfate.

Regarding the methane data, the Slug 3 shows comparatively high concentrations of methane at all the sampling locations. Also, a general trend of decreasing methane concentration in first two sections and increase in the last section is hard to understand. The data shows an increase in methane concentration in the first two sections and decrease in the last section.

The trend for VFA seems to be similar to that observed for methane in general. However, the data for the last section shows increase in VFA concentration for two slugs and decrease in another two. The wastewater pH is relatively constant along the length of the sewer.



Since ferric chloride is dosed in this case, the sulfide present or produced in the biofilm will be precipitated to form iron sulfide precipitates. Calculation of sulfide production rate cannot therefore be done using the sulfide data. Sulfate reduction rate, which gives an indication of sulfide production in the sewer biofilm was therefore calculated based on the measured sulfate data. Similarly, methane production rate and VFA production rate (difference between VFA production and its consumption) were also estimated from the measured data as follows:

$$r_A \left(\frac{g}{m^2 \cdot day} \right) \times \frac{\pi D L(m^2)}{\pi \frac{D^2}{4} L(m^3)} \times HRT(day) = (C_2 - C_1) \left(\frac{g}{m^3} \right)$$

$$r_A = (C_2 - C_1) \times \frac{D}{4} \times \frac{1}{HRT}$$

Calculated sulfate production rates for different sewer sections are shown in Table 8**Error! Reference source not found.**, while VFA and methane production rates are shown in Table 9 and **Error! Reference source not found.** respectively.

Table 8. Sulfate reduction rate in g S/m².day at different sewer sections

Slug	0-2260 m	0-6490 m	2260-6490 m	6490-9894 m	Overall
1	-	-	7.84	0	1.52
2	0	4.13	-	0	1.44
3	0	-	3.62	0	1.09
4	0	-	3.63	0	1.12



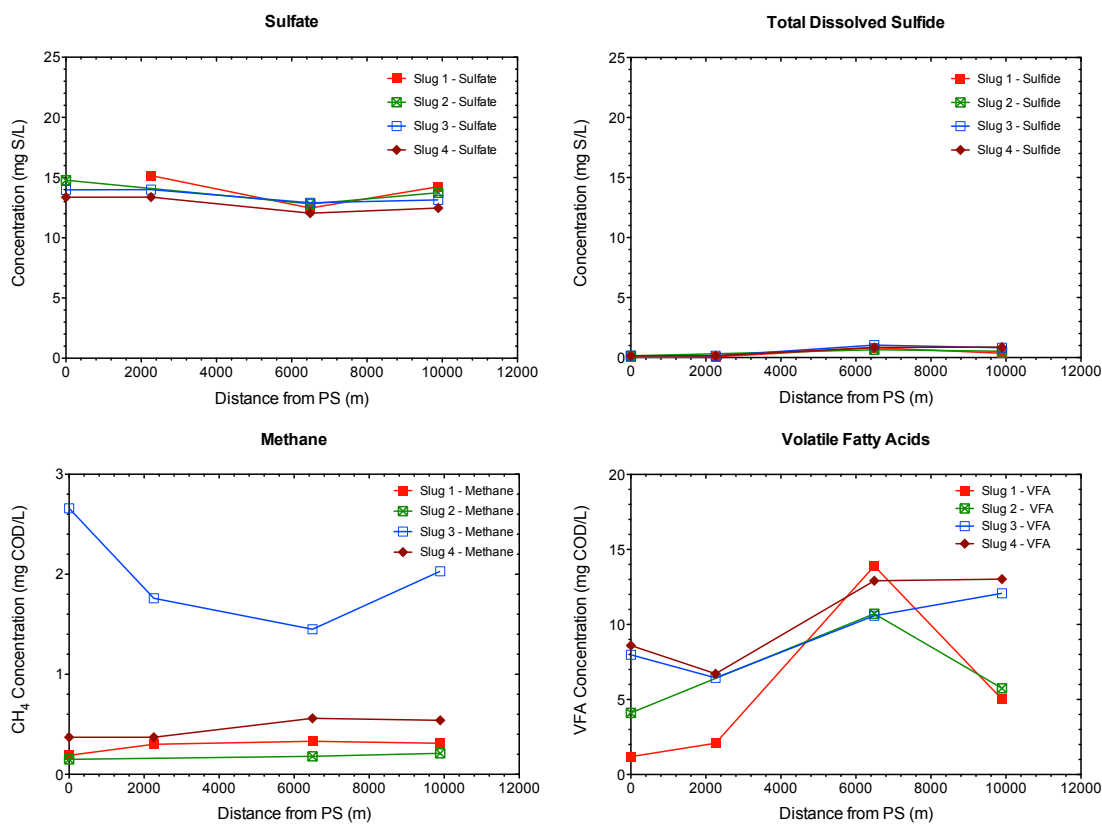


Figure 30. Variation of sulfate, total dissolved sulfide, methane and VFAs along the length of sewer

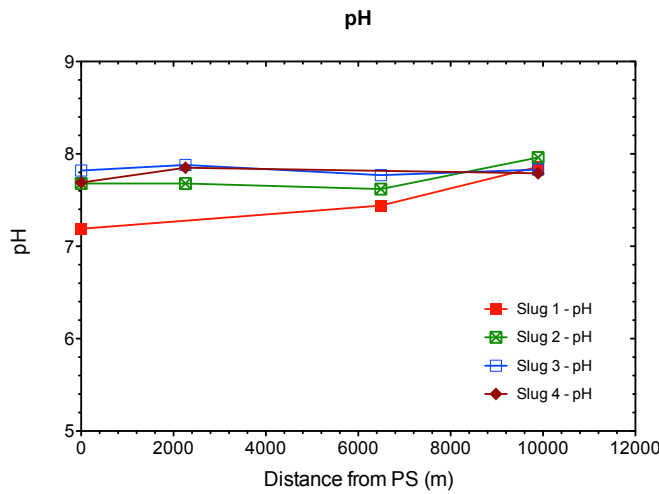


Figure 31. Change in pH along the sewer length

Table 9. VFA production rate in g COD/m².day at different sewer sections

Slug	0-2260 m	0-6490 m	2260-6490 m	6490-9894 m	Overall
1	+4.50	-	+34.50	-33.18	+4.71
2	-	+13.98	-	-19.30	+2.25
3	-10.33	-	+13.58	+4.89	+5.39
4	-10.66	-	+16.81	+0.43	+5.51



Table 10. Methane production rate in g/m².day at different sewer sections

Slug	0-2260 m	0-6490 m	2260-6490 m	6490-9894 m	Overall
1	0.14	-	0	0	0.04
2	-	0	-	0.04	0.02
3	-	-	-	-	-
4	0	-	0.14	0	0.06

As shown in Table 8, sulfide production rate varies at each section of the pipe, and also for each wastewater slug for the same pipe section. Calculation of overall sulfate reduction rate for each wastewater slug shows the sulfate reduction rate to vary between 1.09 to 1.52 g S/m².day, which correspond to 0.83 to 1.05 mg S/L decrease of sulfate concentration. Since no information on the baseline sulfide production rate (production without any chemical dosing) is available, historical data is used for a comparison. Data collected in 2008 from the same system (under similar temperature conditions) showed increase in sulfide concentration to vary from 1.2 to 3.1 mg S/L during the period for which the system was monitored in the current study. This corresponds to average sulfide production rate of 2.0 g S/m².day. Although the sulfide production rate under the ferric dosing (this study) is lower than that observed in the same sewer system without inhibition, the results are somewhat inconclusive owing to the variability of the results, limited amount of data available and lack of baseline data. The contribution of suspended solids is generally ignored in the small systems, but in large pipes such as one in this case, there could be some contribution, which further complicates the calculations. Methane production rates show no methane production in the first section, while there is some production in second section. However, the rate observed here is much lower (2.5 mg /m².h) than the rate reported by Foley et al. (2009), which is 52.4 mg/m².h. Using the model proposed by Foley et al. (2009), methane concentration of 1.02 mg/L is expected, while actual increase in concentration is only 0.05 mg/L. This clearly indicates that methane production was inhibited significantly in the Bellambi sewer system.

3.10. MODELING OF H₂S CONSUMPTION IN SEWER BIOFILM

3.10.1. BACKGROUND

A number of experiments were conducted by SP1 to measure sulfide uptake by the biofilm and relate it to the corrosion activity. These experiments have been undertaken by exposing two different concrete coupons (one was pre-corroded coupon, and the other was fresh coupon) to a reactor with supply of H₂S at certain concentrations, and measuring the gas phase H₂S uptake rate at either 25°C or 30°C. The coupons used in the study were those exposed to the lab-scale controlled chambers for 32 months. SP8 aims to develop a model for estimating the rate of H₂S consumption in biofilm, which will be incorporated in the sewer model to predict accurate H₂S concentration in the gas phase of sewers.

3.10.2. EMPIRICAL MODEL

Empirical models were employed to simulate these four sets of new experimental data, including half order type model, Monod type model and power function type model (as shown below). All the parameters involved in the models were estimated by using MATLAB optimization routine.



1. Half order with respect to gas phase sulfide concentration:

$$r_{H_2S} = k_{max} (S_{H_2S})^{0.5}$$

2. Monod:

$$r_{H_2S} = k_{max} \frac{S_{H_2S}}{S_{H_2S} + K_{H_2S}}$$

3. Power function with respect to sulfide concentration:

$$r_{H_2S} = k_{max} (S_{H_2S})^{\alpha}$$

By using the Monod type model, the parameter of K_{H_2S} (ppm) was overestimated for all the cases, indicating the data could not be described by Monod model. The half order type model could reproduce the measured data reasonably well for all the sets. Figure 32 shows an example of the model simulation results and the measured H_2S concentrations by using the pre-corroded coupon (at 25°C). Estimates of k_{max} in the half order type model are shown in Table 11. By using the power function type model, good fits were achieved between the measured and simulated H_2S gas concentrations for all the sets. Estimates of α in four sets were generally around 0.5 (**Error! Reference source not found.**), which is consistent with the results generated by the half order type model. Figure 33 shows an example of the model simulation results by using the power function type model and the pre-corroded coupon (at 25°C).

Table 11. Estimates of the parameters in the power function model and half order model

Experimental set	Power function model		Half order model
	k_{max}	α	k_{max}
Lab pre-corroded coupon for 32 month (25°C)	96.1	0.6	166.4
Lab pre-corroded coupon for 32 month (30°C)	168.6	0.5	180.6
Lab fresh coupon for 32 month (25°C)	14.9	0.6	26.1
Lab fresh coupon for 32 month (30°C)	32.0	0.5	29.9



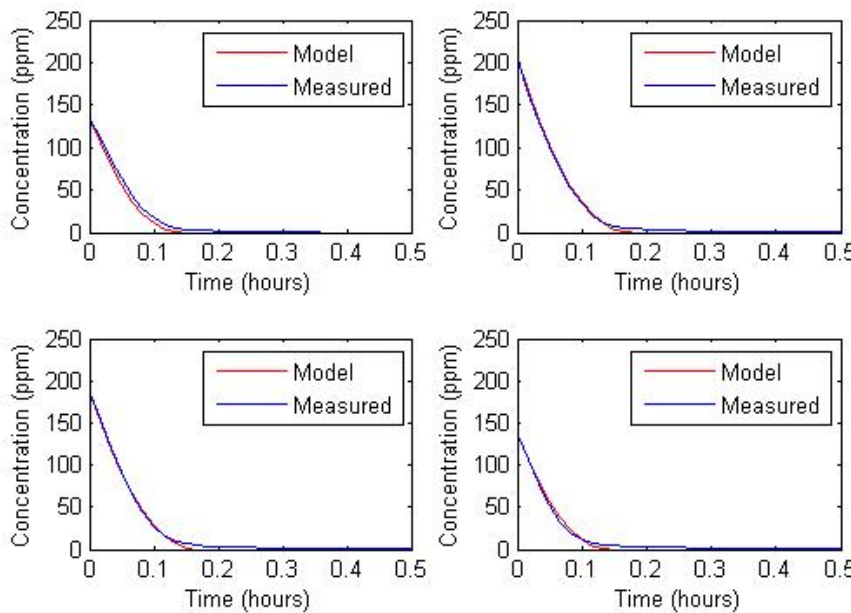


Figure 32. Simulation of H₂S consumption in sewer biofilm by using the half order model against the measured data (the pre-corroded coupon exposed to the lab-scale controlled chamber for 32 months)

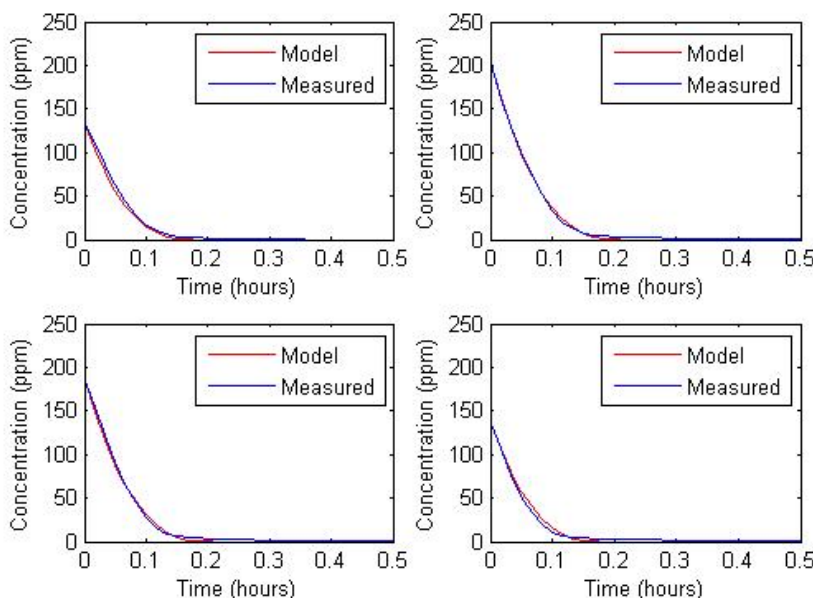


Figure 33. Simulation of H₂S consumption in sewer biofilm by using the power function model against the measured data (the pre-corroded coupon exposed to the lab-scale controlled chamber for 32 months)

3.10.3. FUNDAMENTAL MODEL

A mathematical fundamental model that takes into account the mass transfers of H₂S and O₂ gases and the biological reactions occurred was developed. The chemical reactions were not included in this model, as the surface pH of the tested coupons was between 4 and 5, where the chemical oxidation of H₂S is negligible and hence can be ignored. Influence of gas-liquid mass transfer resistance was considered in this model by including a gas-liquid film

boundary layer. Therefore, the model consisted of a gas-liquid film boundary layer, followed by a liquid film layer. The liquid film layer was divided into a number of small sub-layers to discretize this layer in space. The kinetics of the biological reactions involved in this model was assumed to follow Monod kinetic. The model variables were defined according to the states of gas and liquid film in the experiments (e.g. volume, surface area, concentration, time, etc.). The initial condition used for model estimation and simulation was the initial H₂S gas concentration measured at the beginning of each test. The main output was the profile of H₂S gas concentration in the gas phase.

There were four unknown parameters involved in the fundamental model, including the thickness of boundary layer, the thickness of liquid film layer, maximum sulfide oxidation rate and half saturation constant involved in Monod kinetics. The parameters values were estimated by using MATLAB optimization routine treating all the experimental data in a data set. Generally, the thickness of boundary layer was estimated as 1 μm in all cases (no variation was observed), which was quite small and can be ignored in future. While the thickness of liquid film was estimated about 100 μm, and varying the values of this parameter did not significantly influence the model estimation results as the liquid layer was partially penetrated. Therefore, maximum sulfide oxidation rate (k_{max}) and half saturation constant (K_{H2S}) were the two parameters used to assess and compare the corrosion activity of the tested coupons.

The estimated values for k_{max} and K_{H2S} in each set of experiment are shown in Table 12. The values of k_{max} estimated for the pre-corroded coupons were higher than the values estimated for the fresh coupons. This is consistent as we expected, as the corrosion activity of the liquid film on the pre-corroded coupons should be higher. Based on the estimated parameter values, good fit between the measured and simulated H₂S gas concentrations was obtained for all the experiments. Figure 34 shows an example of the model simulations against the measured data for the lab pre-corroded coupon (at 25°C). The results suggest that the proposed model structure well describes the experimental results.

Table 12. Estimation of the parameters for the fundamental model

Experimental set	k_{max}	K_{H2S}
Lab pre-corroded coupon for 32 month (25°C)	361.7	0.05
Lab pre-corroded coupon for 32 month (30°C)	364.6	0.05
Lab fresh coupon for 32 month (25°C)	34.7	0.10
Lab fresh coupon for 32 month (30°C)	27.2	0.07



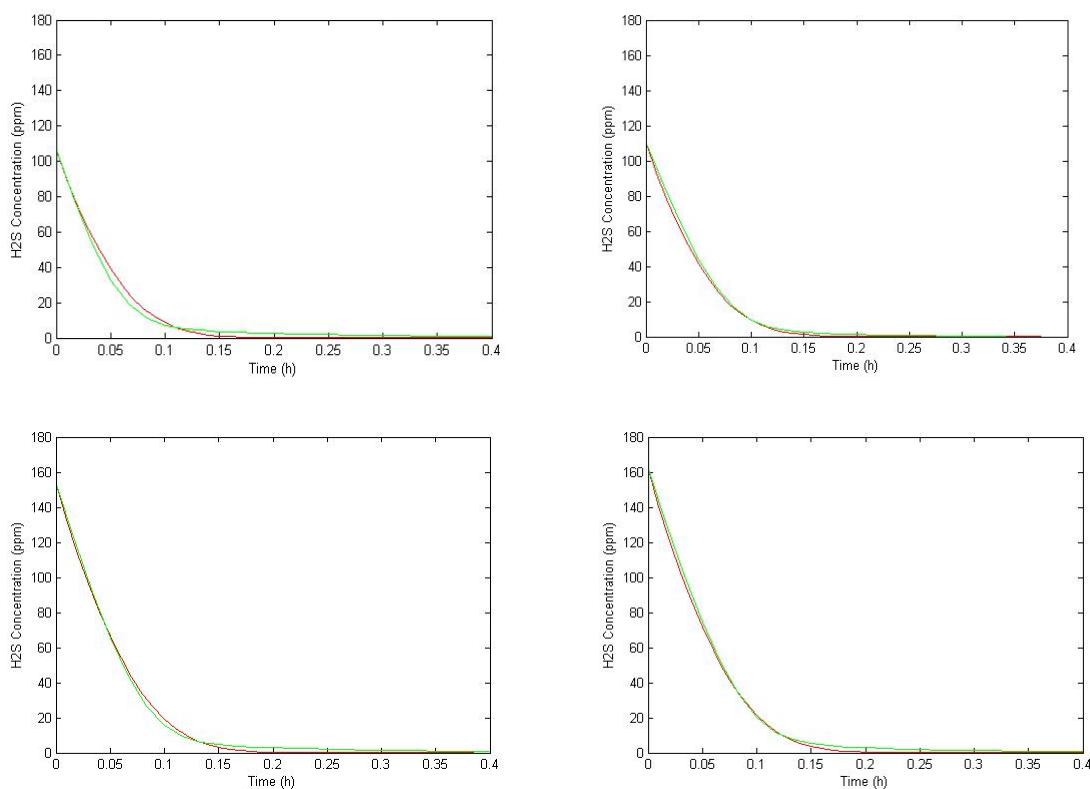


Figure 34. Modelling of H₂S consumption by the liquid film on the surface of a pre-corroded coupon exposed to a lab-scale controlled chamber for 32 months: Comparison of the measured data (green lines) and the model results (red lines)

3.11. SEWER MODELING

3.11.1. IDENTIFICATION OF KEY MODEL PARAMETERS

The sewer model contains a number of parameters to describe the kinetics of processes included in the model. Also, some of these model parameters need to be calibrated for site specific conditions. A sensitivity analysis was conducted to identify the key model parameters.

The following parameters have been identified as the key parameters for the sewer model.

- Temperature coefficient for the biofilm (a_f)
- Temperature coefficient for the bulk phase (a_w)
- Efficiency constant for the water phase (e)
- Hydrogen sulfide production rate constant (k_{H_2S})
- Maximum specific growth rate for heterotrophic biomass (μ_H)
- Maximum rate of fermentation (q_{fe})
- Biomass concentration in the biofilm (X_{Bf})
- Suspended biomass yield constant for heterotrophs (Y_{HW})
- Biofilm yield for heterotrophs (Y_{Hf})

3.11.2. SEWER MODEL UPDATES

The results of the studies reported in this report have been incorporated into the sewer model. The sewer model has been updated with new components as follows:

- Methane production
- Impacts of pH
- Effects of flow velocity
- H₂S transfer in critical structures
- H₂S transfer in gravity sewer pipes
- Effects of dosing of new chemicals
- H₂S uptake by sewer biofilm

3.11.3. IMPACTS OF CHEMICAL DOSING

The following chemicals have been demonstrated to have inhibiting effects on the growth of SRBs and methanogens.

- pH elevation through the dosing of Magnesium Hydroxide
- Shock caustic dosing – intermittent dosing to raise pH above 10.5
- Intermittent FNA dosing (nitrite dosing at a low pH)

Effects of long-term pH change have already been included in the SeweX model (presented in previous technical reports).

The effects of intermittent dosing of chemicals has been modeled as follows:

- A term for the degree of inhibition based on the concentration times the exposure duration (CT value) is included in the model. The correlation between the CT and the degree of inhibition is developed based upon the laboratory and field results.
- Recovery time (time required to reach the maximum biofilm activity after the dosing is stopped) is determined based upon the results of the field study and the laboratory experiments.
- The activity of biofilm is assumed to follow an exponential increase after the dosing is stopped reaching maximum level at the end of the recovery period.

It should be noted here that, the impacts have been modeled based upon the limited data currently available. These modelling components therefore require further enhancements whenever more data becomes available.

3.11.4. DATA IMPORT/EXPORT INTERFACE

The Sewer Model needs dynamic hydraulic data to run. The data can be imported from any hydraulic package that the water industry is currently using. Option of importing data from both the MOUSE and SWMM packages has been included in the model. The outputs from these hydraulic packages vary considerably in terms of data organization and format. For example, data for all the sewer sections can be placed in the same worksheet in MOUSE, while a worksheet of data from SWMM contains all the data for a particular section.



The hydraulic data can be imported either using a MATLAB GUI or using a MATLAB script file. Should there be any other hydraulic package that the industry is currently using, similar data import interface can be developed.

3.11.5. CALIBRATION OF KEY MODEL PARAMETERS

Based on the results of the laboratory and field studies conducted in past several years, and application of sewer model to various sewer systems, the following methodology of calibration is proposed. Please note that the proposed calibration procedure will be further tested in the two model case studies of this project, and will be revised as per the experience gained during the exercise.

Table 13. Summary of proposed calibration methods for model parameter calibration

S.N.	Parameter	Methodology
1	Temperature coefficient for the biofilm (a_f)	<ul style="list-style-type: none"> • A detachable pipe section to be installed on site • Pipe section with mature biofilm to be used as a sewer reactor under hydraulic conditions similar to the real sewer (for details of the sewer pipe and reactor, please refer to Section 4 of the Report on January 2010) • Sulfate reduction rate at temperatures ranging from 10 to 30°C to be measured • Temperature coefficient to be determined from the data
2	Temperature coefficient for the bulk phase (a_w)	<ul style="list-style-type: none"> • Collection of sewage at the end of a sewer pipe • The collected sewage to be used in a completely mixed reactor under constant aeration • COD consumption rate at temperatures ranging from 10 to 30°C to be measured • Temperature coefficient to be determined from the data thus collected
4	Hydrogen sulfide production rate constant (k_{H2S}) Maximum rate of fermentation (q_{fe})	<ul style="list-style-type: none"> • A rising main section without side streams to be selected for monitoring • Feed characteristics and the characteristics of wastewater at the monitoring location to be determined (sulfide, sulfate, VFA)- hourly measurement for 24 hours • Sewer dimensions and pumping data to be collected • Sewer model to be applied to the sewer section • k_{H2S} value to be adjusted to get a good fit between the measured sulfide data and corresponding model predictions • q_{fe} value to be adjusted to get a good fit between the measured VFA data and corresponding model predictions



5	Maximum specific growth rate for heterotrophic biomass (μ_H) Biofilm yield for heterotrophs (Y_{Hf})	<ul style="list-style-type: none"> • Data to be collected from a sewer section with oxygen injection (total and soluble COD, VFA, and DO) • Sewer model based on the sewer properties and hydraulic data • Model to be applied to the system and simulation results to be compared with measured COD, VFA and DO data, • Parameters to be adjusted to achieve a good fit between the measured and model predicted concentrations
7	Biomass concentration in the biofilm (X_{Bf}) Efficiency constant for the water phase (ϵ)	<ul style="list-style-type: none"> • Parameters used to quantify the contribution of sewer biofilm in various biological reactions • These would vary from system to system depending upon the substrate conditions and the sewer hydrodynamics making it extremely difficult to generalize • Default values are recommended unless more accurate information is available
8	Suspended biomass yield constant for heterotrophs (Y_{HW})	<ul style="list-style-type: none"> • Completely mixed reactor operation with sewage collected at the end of a sewer under aeration, • Total and soluble COD measured at a regular interval • Cell COD is measured as the difference between the total COD and soluble COD • Yield coefficient is calculated as the ratio of change in cell COD to the change in soluble COD

3.11.6. AIR TRANSPORT MODELING

A number of approaches to model the air movement in sewers (air transport) were reviewed and a detailed report on this was submitted to TAC. A ventilation model based upon the approach recommended in SP4 has therefore been developed. This model is based upon the steady-state approach, but can be linked to dynamics of sewer flow to predict dynamic changes in the ventilation rate. The output of the ventilation model can then be fed into the sewer model for characterizing the air phase transportation of hydrogen sulfide and other gases.

The model is in the form for a MATLAB® function, which can be called upon to calculate ventilation rates in each section of the pipes in series (sewer network). The function can be employed to normal ventilation conditions as well as the forced ventilation.

Following input data is required for the model:

Sewer properties: roughness coefficients (Manning's roughness coefficient and dry absolute roughness, sewer length, diameter and slope – these to be provided as sewer data



Node properties: Discharge area, discharge coefficient, ground elevation, node discharge elevation, invert levels, wind speed, fan pressure (for forced ventilation)

Hydraulic data: times series of flow rates for each of the sewer sections

Environmental conditions: temperature and relative humidity

The dynamic changes to flow, temperature, relative humidity, and wind speed can be considered by calling the function every time there is change in any of the above parameters.

The ventilation model in its current form can be employed to a sewer network consisting of sewer pipes in series. The model is called upon at every time step to return the airflow rate and velocity for a given section of sewer. The model outputs can then be imported by the main sewer model, which is used to describe transport of hydrogen sulfide and other gases in the air phase.

Major limitations of the approach used in the modeling are:

- The impacts of conditions in the side streams feeding to the trunk main and also the drop structures are ignored.
- Using the steady state approach to deal with a dynamic system will have some implications in terms of mass balances and continuity. Also the transitional phases are ignored.
- The entire sewer network in the cases of large sewer network cannot be modeled at once. The network needs to be broken into smaller networks, which could then be modeled separately.

3.12. MODEL CASE STUDIES

3.12.1. QUEENSBURY SEWER SYSTEM, SA WATER

A sewer model was developed based upon the data collected from the Queensbury Sewer System in Adelaide (SA Water). Intensive sampling campaigns were conducted to collect data for model calibration and validation. Since the sewer receives magnesium hydroxide dosing, the model was first calibrated for magnesium hydroxide dosing. The results of the calibration are presented in Figure 35 and Figure 36. The calibrated model was used to simulate the baseline conditions (without any chemical dosing). In addition, the model was used to optimize the dosing of common chemicals and an economical analysis of chemical dosing options was carried out. In terms of chemical costs, nitrate dosing is found to be the most expensive option, while oxygen injection is more cost-effective compared to the current practice of Mg(OH)₂ dosing in Queensbury.



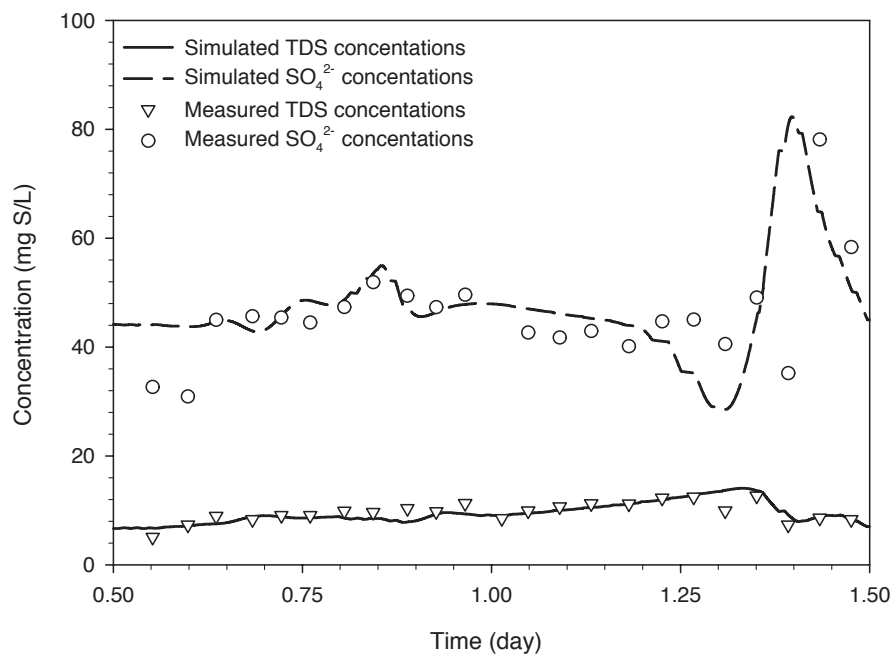


Figure 35. Comparison of measured total dissolved sulfide (TDS) and sulfate levels and model simulated TDS and sulfate levels with magnesium hydroxide addition at the discharge point

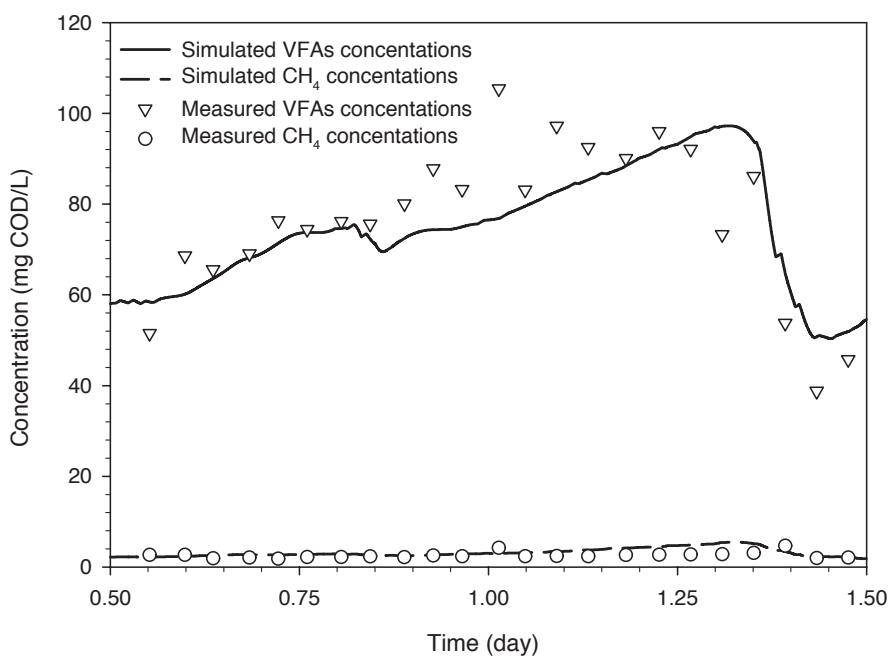


Figure 36. Comparison of measured volatile fatty acids (VFAs) and methane levels and model simulated VFAs and methane levels with magnesium hydroxide addition at the discharge point

The main conclusions of the modelling work are as follows:

- The UQ SeweX model well described the measured data for the Queensbury rising main sewer with magnesium hydroxide addition.

- H₂S discharge from the end of rising mains can be effectively controlled using any of the four chemicals investigated in this study. However, different dosing rates and dosing locations are required for different chemicals.
- The comparison of chemical costs shows that oxygen injection for sulfide control is most cost-effective option.
- This work demonstrates the use of SeweX model as a tool for sewer management. By optimizing the dosing of various chemicals (in terms of both location and dosing rates), the model can be used as a tool for the selection of a cost effect sulfide control strategy.

3.12.2. NSOOS SEWER SYSTEM, SYDNEY WATER

This modelling work, which consists of the modelling of rising main as well as the gravity sewers, has bee completed by Sydney Water. This work demonstrates the application of the SeweX model as well as the ventilation model developed in house by Sydney Water.

3.12.3. VEOLIA WATER SEWER, FRANCE

A sewer system in France (Veolia Water) is being modeled as a case study for the application of the SeweX model. It is a large sewer system consisting of 17 km sewer pipes (combination of gravity and rising main sewers) and 19 pump stations. Veolia Water has provided the data required for the development of the model.

- Sewer details including the layout
- Wastewater characteristics
- Hydraulic data for the sewer pipes
- Temperature data

In terms of data, this sewer system has presented a unique opportunity where the sewer data demands special treatment and some changes to the model have become necessary. Handling of large set of data has made it necessary to develop additional tools for the automation of data compilation. A number of excel macros have been developed for this purpose.

An attempt was made to calibrate the SeweX model based upon the measured hydrogen sulfide data at 6 pump stations. The simulation results using the calibrated model are compared with the measured data in Figure 37.

The sewer system is a network of primarily the gravity sewer sections, in which a number of factors influence the dissolved sulfide as well as the gas phase sulfide concentrations. The key factors are related to liquid gas transfer of gases and the ventilation condition in the sewer system. Since the attempt was made to calibrate the parameters of the model covering these complex processes using a limited number of measurements of hydrogen sulfide, some discrepancies were observed as shown in the figure.

The dissolved sulfide level varied from 1.0 mg S/L to 16.0 mg/L, each sewer showing significant diurnal variation in sulfide level (Figure 38). In some of the rising mains, especially those located at farther upstream of the discharge point (for example the rising mains after the Commandeurs and Estagnol pumping stations) showed consistently higher

dissolved sulfide levels. Other rising mains showed moderate sulfide levels, while few rising mains at pumping station close to the discharge point had lower sulfide levels.

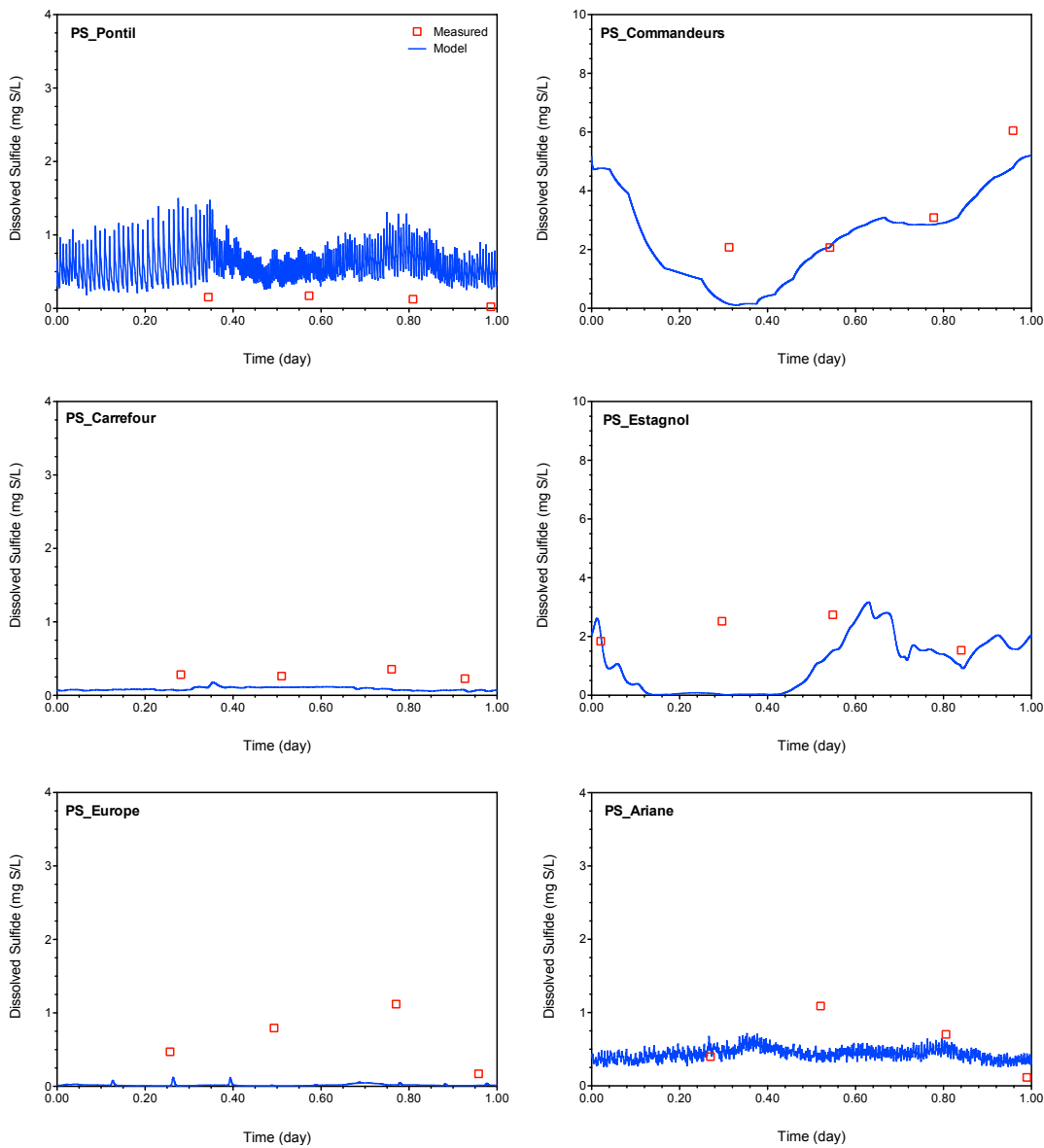


Figure 37. Comparison of simulation results and measured data

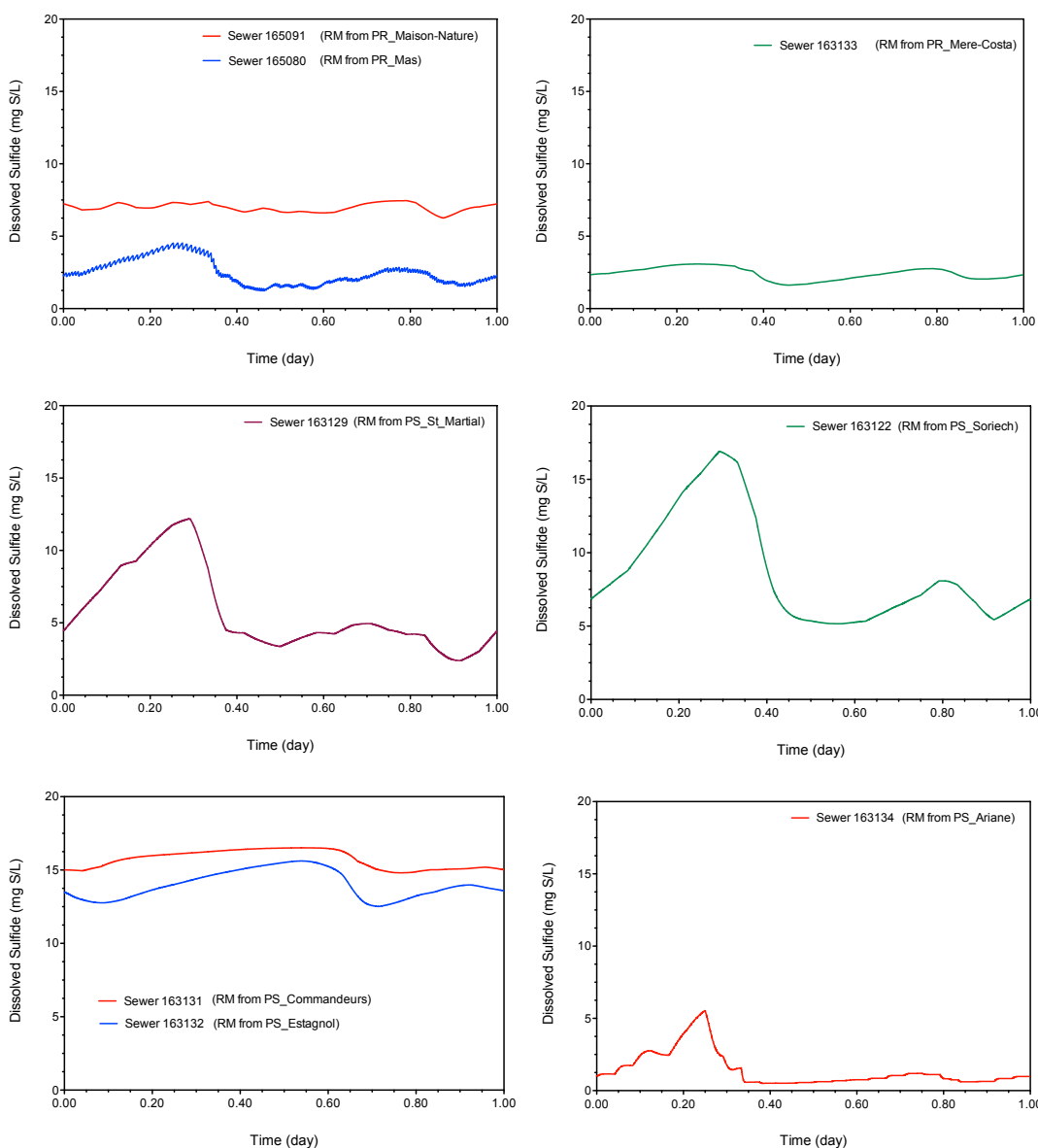


Figure 38. Dissolved sulfide concentration at the end of rising main sections

Based upon the results of the model simulation, potential hotspots for odour and corrosion problem could be identified. The mitigation methods such as chemical dosing to control the production and/or emission of hydrogen sulfide could be designed using the SeweX model. Due to the nature of the sewer network, calibration of the model based upon the measurements in a single rising main and gravity sewer pipes is recommended.

4. REFERENCES

- Balmer, P., Tagizadehnasser, M., 1995. Oxygen-Transfer in Gravity Flow Sewers. Water Science and Technology 31, 127-135.
- Foley J, Yuan Z, Lant P., 2009. Dissolved methane in rising main sewer systems: field measurements and simple model development for estimating greenhouse gas emissions. Water Science and Technology 60(11): 2963-2971.
- Huisman, J., Weber, N., Gujer, W., 2004. Reaeration in sewers. Water Res 38, 1089-1100.
- Jensen, N., 1995. Empirical modeling of air-to-water oxygen transfer in gravity sewers. Water Environ Res 67, 979-991
- Jensen, N., Hvítved-Jacobsen, T., 1991. Method for Measurement of Reaeration in Gravity Sewers Using Radiotracers. Res J Water Pollut C 63, 758-768.
- Krenkel, P., Orlob, G.T., 1962. Turbulent diffusion and the reaeration rate coefficient. Journal of the Sanitary Engineering Division, American Society of Civil Engineers 88, 53-116.
- Krenkel, P., Orlob, G.T., 1962. Turbulent diffusion and the reaeration rate coefficient. Journal of the Sanitary Engineering Division, American Society of Civil Engineers 88, 53-116.
- Lahav, O., Binder, A., Friedler, E., 2006. A different approach for predicting reaeration rates in gravity sewers and completely mixed tanks. Water Environ Res 78, 730-739.
- Siegrist, H., Vogt, D., Garcia-Heras, J. and Gujer, W., 2002. Mathematical model for meso- and thermophilic anaerobic sewage sludge digestion. Environ Sci Technol 36(5), 1113-1123.
- Taghizadeh-Nasser, M., 1986. Gas-liquid mass transfer in sewers (in Swedish), Materieöverföring gas-vätska i avloppsledningar, Chalmers Tekniska Högskola, Göteborg Publikation, p. 3:86.
- Tsivoglou, E., Neal, L., 1976. Tracer Measurement of Reaeration .3. Predicting Reaeration Capacity of Inland Streams. Journal Water Pollution Control Federation 48, 2669-2689.
- Zytner, R., MadanilSfahani, M., Corsi, R., 1997. Oxygen uptake and VOC emissions at enclosed sewer drop structures, Water Environ Res, pp. 286-294.

